ity bias. The task comprises 10 short vignettes presenting an interaction between a fictional character and the study participant. Each vignette was read aloud by the tester. If the subject requested, the vignette was repeated once. The tester then had the subject respond 'Yes' or 'No' to three questions about the vignette, addressing verbal memory, schematic inference, and ToM. ToM items were designed to assess both ToM and hostile attributional bias. Questions were presented in a random order, and subjects were then asked to rate their confidence level in their answer to the last question.

Scoring for the verbal memory, schematic inference and ToM subscales reflected the sum of correct answers (range 0–10; higher scores indicate better performance). Scoring for the hostility bias scale was the sum of instances in which the subject erroneously inferred that the vignette character had negative thoughts or feelings toward the subject (range 0–5; higher scores indicate greater bias). As for the metacognition scores, if the subject answered correctly on the last question, a score of 1 was given; if the subject answered incorrectly on the last question a score of 0 was given if he/she answered that he/she was 'very sure', 0.33 for 'pretty sure', 0.66 for 'a little unsure', and 1 for 'not sure at all'. The metacognition score was obtained by summing up the scores for the 10 vignettes (range 0–10; higher scores indicate better metacognitive ability). The total score was calculated as the sum of all the subscales except for hostility bias scale because the items used for calculating the scores overlapped with those used for ToM scores. The SCSQ was administered to both schizophrenia and normal control subjects (see Appendix S1 for a sample item).

AIHQ

Attributional bias was assessed using the AIHQ.[18] Subjects read a series of 15 vignettes describing social situations with negative outcomes and answered questions about the intentions of the characters and how subjects themselves would respond to the situation. The vignettes involved three categories of situations, which were considered to be 'accidental', 'intentional', or 'ambiguous' in terms of the cause of the negative outcomes. Following Combs *et al.*,[18] we focused on scores of ambiguous situations for analyses and computed three summary scores: hostility bias, aggression bias, and blame scores (see Appendix S2 for a sample item).

Hinting Task

The Hinting Task is a measure of ToM. Subjects are required to infer real intentions behind indirect speech.[12] The task comprises 10 short passages presenting an interaction between two characters ending with one of the characters uttering a hint. Each passage was read aloud by the tester. The subject was then asked what the character really meant when he/she uttered the hint. If the subject failed to give the correct response, an even more obvious hint was added to the story and the subject was asked again. A correct response was therefore scored as 2 or 1, depending on when the response was given. The score was obtained by summing the score for each response (see Appendix S3 for a sample item).

BCIS

The BCIS is a measure of cognitive insight, which is linked to metacognition. It measures the extent to which subjects agree with statements pertaining to how certain they are of the accuracy of their judgments. Two subscale scores are produced: self-reflectiveness and self-certainty. While higher scores on the former indicate higher level of cognitive insight, higher scores on the latter indicate lower level of cognitive insight.[15] A composite score obtained by subtracting the self-certainty scores from the self-reflectiveness scores was adopted for analysis. The Japanese version of the BCIS was validated in a previous study.[16] As some questions are related to insight about mental illness, the BCIS was administered only to schizophrenia patients.

Social functioning

We adopted the SFS developed by Birchwood *et al.*,[19] which is a measure assessing social functioning across seven domains: (i) social engagement; (ii) interpersonal communication; (iii) independence-performance; (iv) recreation; (v) social activities; (vi) independence-competence; and (vii) occupation (with higher scores indicating a higher level of functioning). The domain score was computed by summing the item scores in each domain. The total score was the sum of seven domain scores. In the present study, we used self-report rather than informant interview for only the schizophrenia patients.

Statistical analysis

A Mann–Whitney–Wilcoxon rank sum test was used to explore between-group differences for SCSQ subscale scores and Hinting Task scores. As the subjects were neither allowed to read the task sentences themselves nor hear the task sentences more than twice, SCSQ subscale scores may well be affected by verbal memory ability. Therefore, if a significant between-group difference in verbal memory was found, a one-way ANCOVA using subscale scores of verbal memory in the SCSQ as a covariate was performed for each subscale's scores to test the effect of group. To examine between-group differences in AIHQ scores, we conducted a mixed model ANOVA with three situations (intentional, ambiguous, and accidental) as a within-subjects factor, group as a between-subjects factor, and each subscale's scores of AIHQ (hostility bias, blame score, and aggression bias) as dependent measures. Secondary analyses were performed whenever a significant interaction between the factors was obtained. In addition, in order to estimate the sensitivity and specificity of the SCSQ total score in distinguishing patients from normal controls, we set a cut-off score based on receiver–operator curve (ROC) analysis.

As for internal consistency, we excluded hostility bias to avoid redundancy because the items used to calculate the score overlapped with those used in ToM scores. Cronbach's alpha was thus calculated using the four subscales.

Spearman's rho was calculated for the schizophrenia patients to examine the correlation of the SCSQ subscale scores and other indices to investigate the SCSQ's convergent, discriminant and ecological validity.

We hypothesized that schizophrenia patients should score significantly lower in the SCSQ subscales and the Hinting Task, and higher in the AIHQ subscales in ambiguous situations than normal controls. In terms of the construct validity of the SCSQ, we hypothesized that there should be positive correlations among the following: (i) SCSQ ToM subscale and the Hinting Task scores, but not between SCSQ schematic inference subscale scores and Hinting Task scores; (ii) SCSQ hostility bias and AIHQ hostility, aggression bias, and blame scores; (iii) SCSQ metacognition subscale scores and BCIS composite scores; and (iv) social cognitive subscale scores of the SCSQ and SFS scores.

RESULTS

Between-group comparison of social cognition

SCSQ

There were significant between-group differences for all SCSQ subscales and the total scores (Table 2). As there was a significant between-group difference in the verbal memory subscale, one-way ANCOVA using the verbal memory subscale's scores as a covariate was performed for each subscale's scores. The main effects of group remained significant for schematic inference ($F\ [1,\ 103] = 24.49$, $P < 0.0001$), ToM ($F\ [1,\ 103] = 50.05$, $P < 0.0001$), metacognition ($F\ [1,\ 103] = 6.43$, $P < 0.05$), hostility bias ($F\ [1,\ 103] = 10.75$, $P < 0.005$) and total scores ($F\ [1,\ 104] = 71.94$, $P \leq 0.0001$), indicating that these differences were present above and beyond the effects of verbal memory impairment in schizophrenia.

The ROC analysis for the total score indicated that a cut-off point of 34.0 would provide a sensitivity of 0.87 and a specificity of 0.69. Moreover, the area under the ROC was 0.84.

AIHQ

Hostility bias: A mixed model ANOVA revealed a significant main effect of situation ($F\ [2, 206] = 192.45$, $P < 0.0001$, G-G corrected), and a significant interaction between group and situation ($F\ [2, 206] = 12.83$, $P < 0.0001$, G-G corrected). A secondary analysis for each situation revealed a significant main effect of group only in the intentional situations. Hostility bias was stronger in normal controls compared with schizophrenia patients in intentional situations (Table 2).

Blame score: There was a significant main effect of situation ($F\ [2, 206] = 253.46$, $P < 0.0001$, G-G corrected), and a significant interaction between group and situation ($F\ [2, 206] = 8.29$, $P < 0.001$, G-G corrected). Similar to the hostility bias scale, the blame score was stronger in normal controls compared with schizophrenia patients in intentional situations (Table 2).

Aggression bias: There was a significant main effect of situation ($F\ [2,\ 206] = 13.47$, $P < 0.0001$); however, there was neither a significant effect of group ($F\ [1103] = 0.14$, not significant [NS]) nor a significant interaction between group and situation ($F\ [2, 206] = 1.58$, NS) (Table 2).

Table 2. Between-group comparison of SCSQ and AIHQ subscale scores

	Schizophrenia ($n = 52$)	Normal controls ($n = 53$)	Between-group comparison
SCSQ			
Verbal memory	7.92 (1.13)†	8.64 (0.86)	$Z = -3.57$, $P < 0.001$
Schematic inference	7.54 (1.35)	8.60 (0.91)	$Z = -4.31$, $P < 0.0001$
Theory of mind	6.56 (1.51)	8.43 (1.38)	$Z = -6.08$, $P < 0.0001$
Metacognition	9.22 (0.64)	9.50 (0.53)	$Z = 2.43$, $P < 0.05$
Hostility bias	1.52 (1.09)	0.89 (0.91)	$Z = -3.08$, $P < 0.01$
Total	31.24 (3.47)	35.08 (2.52)	$Z = -5.99$, $P < 0.0001$
AIHQ			
Hostility bias			
Intentional	1.93 (0.41)	2.19 (0.40)	$Z = -3.68$, $P < 0.001$
Ambiguous	1.71 (0.46)	1.59 (0.32)	NS
Accidental	1.30 (0.33)	1.25 (0.20)	NS
Blame score			
Intentional	3.23 (0.75	3.54 (0.55)	$Z = -2.44$, $P < 0.05$
Ambiguous	2.49 (0.71)	2.34 (0.48)	NS
Accidental	2.13 (0.64)	2.09 (0.41)	NS
Aggression bias			
Intentional	1.77 (0.64)	1.82 (0.52)	NS
Ambiguous	1.75 (0.61)	1.69 (0.32)	NS
Accidental	1.61 (0.64)	1.51 (0.40)	NS
Hinting Task	14.02 (3.67)	16.23 (3.07)	$Z = -3.34$, $P < 0.001$

†Mean (SD).
AIHQ, Ambiguous Intentions Hostility Questionnaire; NS, not significant; SCSQ, Social Cognition Screening Questionnaire.

Hinting Task

Schizophrenia patients scored significantly lower than normal controls on the Hinting Task (Table 2).

Internal consistency

Cronbach's alpha for the SCSQ total score, including verbal memory, schematic inference, ToM and metacognition, was 0.72.

Convergent and discriminant validity

Construct validity findings are summarized in Tables 3 and 4. Regarding ToM, a significant correlation was obtained between the SCSQ ToM subscale and the Hinting Task. Regarding hostility bias, there was a significant correlation between the SCSQ hostility bias and the AIHQ hostility bias, blame scores, and aggression bias. Regarding metacognition, there was a significant correlation between the SCSQ metacognition subscale and the BCIS composite scale. There were also significant negative correlations between SCSQ ToM subscale and the AIHQ blame scores and aggression bias, and also between SCSQ verbal memory subscale and AIHQ aggression bias. Finally, the SCSQ schematic inference subscale did not correlate with any measures of social cognition except for a weak negative correlation with the AIHQ blame scores.

Ecological validity

As for the relation between the SCSQ and social functioning, ToM subscale scores showed significant positive correlations with the scores of four domains of social functioning, including social engagement, interpersonal communication, recreation, and occupation; metacognition subscale scores showed positive correlations with the domain scores of recreation and occupation; hostility bias subscale scores were negatively correlated with the domain score of social

Table 3. Spearman's rho between SCSQ scores and other social cognition measures

	Verbal memory	Schematic inference	Theory of mind	Metacognition	Hostility bias	Total
Hinting Task	0.35*	0.25	0.52****	0.13	−0.25	0.48***
BCIS						
Composite	−0.10	0.10	0.22	0.32*	0.19	0.20
AIHQ (ambiguous)						
Hostility	0.12	−0.05	−0.06	0.24	0.34*	0.03
Blame	−0.25	−0.28*	−0.42**	−0.17	0.47***	−0.42**
Aggression	−0.31*	−0.26	−0.45***	−0.02	0.37**	−0.35*

****$P < 0.0001$. ***$P < 0.001$. **$P < 0.01$. *$P < 0.05$.
AIHQ, Ambiguous Intentions Hostility Questionnaire; BCIS, Beck Cognitive Insight Scale; SCSQ, Social Cognition Screening Questionnaire.

engagement; total scores were positively correlated with the domain score of occupation (Table 4).

DISCUSSION

Between-group differences

The SCSQ showed more robust between-group differences than our other measures of social cognition, the AIHQ and the Hinting Task. A recent meta-analysis showed that patients with schizophrenia performed worse than normal controls across all domains of social cognition, with a relatively large effect size shown in social perception (1.04), ToM (0.96), and emotion processing (0.89).[23] In the present study, the effect size of SCSQ ToM subscale scores (1.36) exceeded both the effect size of ToM in the above study and of the Hinting Task in the present study (0.72). As for attributional bias, the effect size shown for SCSQ hostility bias was 0.69, whereas none of the AIHQ scores in ambiguous situations showed a significant between-group difference. Moreover, the total score distinguished the patients from normal controls with a sensitivity of 0.87 and a specificity of 0.69 and the area under the ROC was 0.84, which indicated a high level of discrimination. Thus, the robust between-group differences in the subscales of ToM and hostility bias and the total score in the SCSQ provide support for the sensitivity and construct validity of these subscales.

Table 4. Spearman's rho between SCSQ and SFS subscale scores

	Verbal memory	Schematic inference	Theory of mind	Metacognition	Hostility bias	Total
SFS	0.03	0.10	0.23	0.08	−0.22	0.11
Total score						
Social engagement	0.00	0.10	0.33*	0.16	−0.29*	0.27
Interpersonal communication	0.14	−0.01	0.41**	0.18	−0.18	0.26
Independence-performance	−0.09	0.02	−0.04	−0.13	−0.08	−0.12
Recreation	−0.01	0.01	0.38**	0.30*	−0.13	0.22
Social activities	0.12	0.18	0.15	0.08	−0.22	0.16
Independence-competence	−0.08	0.02	0.01	−0.12	−0.11	−0.12
Occupation	0.17	0.04	0.46***	0.29*	−0.22	0.32*

***$P < 0.001$. **$P < 0.01$. *$P < 0.05$.
SCSQ, Social Cognition Screening Questionnaire; SFS, Social Functioning Scale.

We found a weak but significant between-group difference in the metacognition subscale, which was in line with the previous research[24] measuring the participants' confidence level in error responses to the 'Reading the mind in the eyes test', indicating that the patients committed more high-confidence errors than did healthy controls. In the present study, metacognitive ability was, at least in part, evaluated using confidence level to the error responses, which might have led to the similar result.

Internal consistency

Cronbach's alpha for the SCSQ total score was 0.72, which was considered acceptable. Considering that social cognition is a multifaceted concept and the scale covers different dimensions and that panelists in a recent RAND panel agreed not to consider Cronbach's alpha as a criterion for evaluation of social cognitive measures,[25] the significance of the value is not necessarily clear. However, we consider that the value is acceptable to use the SCSQ total score summing up these subscale scores.

Convergent and discriminant validity

We found that the SCSQ ToM subscale scores showed a relatively strong relation with the Hinting Task scores, which supports the SCSQ's convergent validity. Both tasks require the subjects to characterize the mental states of other people and to modify their responses by projecting oneself imaginatively into the 'mental shoes' of another person in an interpersonal situation.[26] In contrast, the SCSQ schematic inference subscale scores did not significantly correlate with the Hinting Task scores. Although both the SCSQ ToM and schematic inference subscales require the subjects to make inferences from uncertain and ambiguous context information, the latter does not involve mentalizing, which is associated with the SCSQ ToM subscale and the Hinting Task. The lack of a significant correlation between the SCSQ schematic inference subscale and the Hinting Task supports the view that the key element that links the SCSQ ToM subscale and the Hinting Task may be the process of mentalizing. Moreover, we found a significant negative correlation between SCSQ ToM subscale scores and scores of AIHQ blame scores and aggression bias. Although we did not a priori expect these relations, considering that poor ToM leads to a misunderstanding of another's intent, together with personalizing bias, it is not difficult to presume that it may cause exaggerated blame and aggression to others. An alternative explanation is that because the SCSQ ToM and hostility bias scales are based on the same response set, it is possible that, for some participants, poor ToM performance was caused by high hostility bias rather than by diminished mentalizing capacity.

We also found SCSQ hostility bias scores significantly correlated with scores of AIHQ hostility, aggression bias, and blame scores in ambiguous situations, as expected. Both tasks require subjects to judge the intention of characters in short, ambiguous vignettes, which may have contributed to the significant relation between the scores in the two tests. Moreover, as 'blame score' and 'aggression bias' are well assumed to be related to 'hostility bias' in the AIHQ, it is unsurprising to find a significant correlation between SCSQ hostility bias and AIHQ blame scores and aggression bias.

There was a significant but modest correlation between SCSQ metacognition and BCIS composite scores. The SCSQ is a performance-based measure while the BCIS is a self-report measure, which may have led to the modest level of correlation. In a previous study investigating the relation between BCIS scores and confidence level of error responses to the 'Reading the mind in the eyes test', along with a positive correlation between BCIS self-certainty scores and the confidence level to error responses, a *positive* correlation was unexpectedly demonstrated between self-reflective scores and the confidence level to error responses.[24] Although we found a significant positive correlation between SCSQ metacognition subscale scores and BCIS composite scores as expected, the level of correlation was modest. We should carefully consider the metacognitive dissonance between subjective and objective social cognition abilities; it may happen that the patients think they are more self-critical, although in fact they show greater overconfidence in errors.

Ecological validity

Social cognition has been identified as a contributor to functional outcome because the ability to process social stimuli is essential for social interactions and thus affects interpersonal relationships with others in the community as well as work and school behavior.[3] In several recent studies, it has been demonstrated that social cognition serves as a

mediator between neurocognition and social functioning.[4–7,27,28] Therefore, we predicted that the subscale scores of the SCSQ would correlate with the scores of social functioning measured by the SFS. We found a significant positive correlation between SCSQ ToM subscale and the four domains of social functioning, including social engagement, interpersonal communication, recreation, and occupation, and also positive correlations between the SCSQ metacognition subscale and the two SFS domains, such as recreation and occupation, and a negative correlation between the SCSQ hostility bias and the domain of social engagement. As for the SCSQ total score, we found only a modest correlation with the domain score of occupation, which suggests that the ToM subscale is more closely related to social functioning than the SCSQ total score. This finding may relate to evidence that social cognition is more closely linked to social functioning and the total score includes verbal memory, which is more neurocognitive and thus may dilute the association to social functioning. Although most previous studies examining the relation between social cognition and social functioning used emotion and social perception measures of social cognition, a few studies have demonstrated a significant relation between ToM, metacognition, attributional bias, and functional outcome.[28–31] For example, Couture *et al.*[28] demonstrated that ToM as indexed by the Hinting Task partially mediated the relation between neurocognition and social competence. Our study results support the ecological validity of the SCSQ, and also the continued use of subscale scores rather than just the total score.

Limitations

There are several limitations of the present study that should be addressed. First, as we lack validated standard measures for assessing social cognition in the adult psychiatric population in Japan, we selected the measures for investigating the criterion-related validity of the SCSQ under the following conditions: (i) the original version of the test had been validated; (ii) the criteria were not greatly affected by cultural differences; (iii) the test was assumed to tap similar domains of social cognition as the SCSQ. Although both the Hinting Task and the AIHQ are validated in their original forms, neither of the Japanese translation versions has yet been validated. However, except for a few points in the AIHQ, we found it unnecessary to change the content of these measures to fit Japanese culture. The few points in the AIHQ concerned settings that were rather unusual in Japan. Through discussion with Dr Combs, who developed the AIHQ, we replaced them with settings more natural and appropriate for Japanese culture. The fact that we obtained significant relations between the SCSQ ToM subscale and the Hinting Task, and also between hostility bias of the SCSQ and hostility bias, blame scores and aggression bias of the AIHQ in ambiguous situations, provides some initial support for the validity of the Japanese versions of both the Hinting Task and the AIHQ.

Second, our sample size was small, and included participants of a wide range of age, illness duration, and symptom profiles. These demographic factors could have different effects on social cognition and a greater sample size may enable us to investigate the effect of various demographics as well as clinical factors.

Third, to apply the SCSQ in clinical trials targeting social cognition, we need to confirm its test–retest reliability, which was not evaluated in the present study. Given the current study's support for the construct validity of the SCSQ ToM and hostility bias subscales, we are now planning to investigate the test–retest reliability in the near future.

Conclusion

Based on these results, the SCSQ subscales appeared to be valid measures. The construct validity evidence for the SCSQ supports its use as a novel measure of ToM, metacognition and hostility bias.

ACKNOWLEDGMENTS

This study was funded by the Intramural Research Grant (21-1) for Neurological and Psychiatric Disorders of NCNP. There are no conflicts of interest for any of the authors of this paper. No author has any possible financial gain for the findings presented here. We thank Prof. Nishikawa (Tokyo Medical and Dental University) for his helpful advice. [Correction added on 6 June 2014, after first online publication: The authors added another acknowledgment.]

REFERENCES

1. Regier DA, Narrow WE, Rae DS, Manderscheid RW, Locke BZ, Goodwin FK. The de facto US mental and addictive disorders service system. Epidemiologic Catchment Area

prospective 1-year prevalence rates of disorders and services. *Arch. Gen. Psychiatry* 1993; 50: 85–94.
2. Couture SM, Penn DL, Roberts DL. The functional significance of social cognition in schizophrenia: A Review. *Schizophr. Bull.* 2006; 32 (Suppl. 1): 44–63.
3. Brekke J, Kay DD, Lee KS, Green MF. Biosocial pathways to functional outcome in schizophrenia. *Schizophr. Res.* 2005; 80: 213–225.
4. Addington J, Saeedi H, Addington D. Facial affect recognition: A mediator between cognitive and social functioning in psychosis. *Schizophr. Res.* 2006; 85: 142–150.
5. Addington J, Saeedi H, Addington D. Influence of social perception and social knowledge on cognitive and social functioning in early psychosis. *Br. J. Psychiatry* 2006; 189: 373–378.
6. Schmidt SJ, Mueller DR, Roder V. Social cognition as a mediator variable between neurocognition and functional outcome in schizophrenia: Empirical review and new results by structural equation modeling. *Schizophr. Bull.* 2011; 37 (Suppl. 2): 41–54.
7. Adolphs R. The social brain: Neural basis of social knowledge. *Annu. Rev. Psychol.* 2009; 60: 693–716.
8. Ochsner KN. The social-emotional processing stream: Five core constructs and their translational potential for schizophrenia and beyond. *Biol. Psychiatry* 2008; 64: 48–61.
9. Green MF, Olivier B, Crawley JN, Penn DL, Silverstein S. Social cognition in schizophrenia: Recommendations from the Measurement and Treatment Research to Improve Cognition in Schizophrenia New Approaches Conference. *Schizophr. Bull.* 2005; 31: 882–887.
10. Roberts DL, Fiszdon J, Tek C. Initial validity of the Social Cognition Screening Questionnaire (SCSQ). *Schizophr. Bull.* 2011; 37 (Suppl. 1): 280.
11. Premack D, Woodruff G. Does the chimpanzee have a theory of mind? *Behav. Brain Sci.* 1978; 4: 515–526.
12. Corcoran R, Mercer G, Frith CD. Schizophrenia, symptomatology and social inference: Investigating theory of mind in people with schizophrenia. *Schizophr. Res.* 1995; 17: 5–13.
13. Garety PA, Freeman D. Cognitive approaches to delusions: A critical review of theories and evidence. *Br. J. Clin. Psychol.* 1999; 38: 113–154.
14. Moritz S, Woodward TS. A generalized bias against disconfirmatory evidence in schizophrenia. *Psychiatry Res.* 2006; 142: 157–165.
15. Beck AT, Baruch E, Balter JM, Steer RA, Warman DM. A new instrument for measuring insight: The Beck Cognitive Insight Scale. *Schizophr. Res.* 2004; 68: 319–329.
16. Uchida T, Matsumoto K, Kikuchi A *et al.* Psychometric properties of the Japanese version of the Beck Cognitive Insight Scale: Relation of cognitive insight to clinical insight. *Psychiatry Clin. Neurosci.* 2009; 63: 291–297.
17. Martin JA, Penn DL. Attributional bias in schizophrenia: An investigation in outpatients with and without persecutory delusions. *Schizophr. Bull.* 2002; 28: 131–141.
18. Combs DR, Penn DL, Wicher M, Waldheter E. The Ambiguous Intentions Hostility Questionnaire (AIHQ): A new measure for evaluating hostile social-cognitive biases in paranoia. *Cogn. Neuropsychiatry* 2007; 12: 128–143.
19. Birchwood M, Smith J, Cochrane R, Wetton S, Copestake S. The Social Functioning Scale. The development and validation of a new scale of social adjustment for use in family intervention programmes with schizophrenic patients. *Br. J. Psychiatry* 1990; 157: 853–859.
20. Social Cognition and Interaction. Training program for schizophrenia spectrum disorders. *Psychiatr. Serv.* 2007; 58: 449–451.
21. Matsuoka K, Uno M, Kasai K, Koyama K, Kim Y. Estimation of premorbid IQ in individuals with Alzheimer's disease using Japanese Ideographic script (kanji) compound words: Japanese version of National Adult Reading Test. *Psychiatry Clin. Neusosci.* 2006; 60: 332–339.
22. Kay SR, Fiszbein A, Opler LA. The Positive and Negative Syndrome Scale (PANSS) for schizophrenia. *Schizophr. Bull.* 1987; 13: 261–276.
23. Savla GN, Vella L, Armstrong CC, Penn DL, Twamley EW. Deficits in domains of social cognition in schizophrenia: A meta-analysis of the empirical evidence. *Schizophr. Bull.* 2012; 39: 979–992.
24. Köther U, Veckenstedt R, Vitzthum F *et al.* "Don't give me that look" – Overconfidence in false mental state perception in schizophrenia. *Psychiatry Res.* 2012; 196: 1–8.
25. Pinkham AE, Penn DL, Green MF, Buck B, Healey K, Harvey PD. The Social Cognition Psychometric Evaluation Study: Results of the Expert Survey and RAND Panel. *Schizophr. Bull.* 2014; 40: 813–823.
26. Diamond MD. The ability of schizophrenics to modify responses in an interpersonal situation. *J. Consult. Psychol.* 1956; 20: 441–444.
27. Sergi MJ, Rassovsky Y, Nuechterlein KH, Green MF. Social perception as a mediator of the influence of early visual processing on functional status in schizophrenia. *Am. J. Psychiatry* 2006; 163: 448–454.
28. Couture SM, Granholm EL, Fish SC. A path model investigation of neurocognition, theory of mind, social competence, negative symptoms and real-world functioning in schizophrenia. *Schizophr. Res.* 2011; 125: 152–160.
29. Lysaker PH, Lancaster RS, Nees MA, Davis LW. Attributional bias and symptoms as predictors of social function in schizophrenia. *J. Rehabil. Res. Dev.* 2004; 41: 225–232.
30. Roncone R, Falloon IR, Mazza M *et al.* Is theory of mind in schizophrenia more strongly associated with clinical and social functioning than with neurocognitive deficits? *Psychopathology* 2002; 35: 280–288.
31. Koren D, Seidman LJ, Goldsmith M, Harvey PD. Real-world cognitive – and metacognitive – dysfunction in schizophrenia: A new approach for measuring (and remediating) more 'right stuff'. *Schizophr. Bull.* 2006; 32: 310–326.

SUPPORTING INFORMATION

Additional Supporting Information may be found in the online version of this article at the publisher's web-site:

Appendix S1. Sample item of Social Cognition Screening Questionnaire.
Appendix S2. Sample item of Ambiguous Intentions Hostility Questionnaire; ambiguous situation.
Appendix S3. Sample item of Hinting Task.

Behavioral/Cognitive

Topographic Representation of an Occluded Object and the Effects of Spatiotemporal Context in Human Early Visual Areas

Hiroshi Ban,[1,2,3] Hiroki Yamamoto,[3] Takashi Hanakawa,[4] Shin-ichi Urayama,[5] Toshihiko Aso,[5] Hidenao Fukuyama,[5] and Yoshimichi Ejima[6]

[1]Center for Information and Neural Networks, National Institute of Information and Communications Technology, Osaka, 565-0871, Japan, [2]The Japan Society for the Promotion of Science, Tokyo 102-8472, Japan, [3]Graduate School of Human and Environmental Studies, Kyoto University, Yoshida-Nihonmatsu-Cho, Sakyo-ku, Kyoto City, Kyoto 606-8501, Japan, [4]National Center of Neurology and Psychiatry, Tokyo 187-8502, Japan, [5]Human Brain Research Center, Graduate School of Medicine, Kyoto University, Yoshida-Konoe-Cho, Sakyo-Ku, Kyoto City, Kyoto 606-8507, Japan, and [6]Kyoto Institute of Technology, Matsugasaki Hashikami-Cho, Sakyo-Ku, Kyoto City, Kyoto 606-8585, Japan

Occlusion is a primary challenge facing the visual system in perceiving object shapes in intricate natural scenes. Although behavior, neurophysiological, and modeling studies have shown that occluded portions of objects may be completed at the early stage of visual processing, we have little knowledge on how and where in the human brain the completion is realized. Here, we provide functional magnetic resonance imaging (fMRI) evidence that the occluded portion of an object is indeed represented topographically in human V1 and V2. Specifically, we find the topographic cortical responses corresponding to the invisible object rotation in V1 and V2. Furthermore, by investigating neural responses for the occluded target rotation within precisely defined cortical subregions, we could dissociate the topographic neural representation of the occluded portion from other types of neural processing such as object edge processing. We further demonstrate that the early topographic representation in V1 can be modulated by prior knowledge of a whole appearance of an object obtained before partial occlusion. These findings suggest that primary "visual" area V1 has the ability to process not only visible or virtually (illusorily) perceived objects but also "invisible" portions of objects without concurrent visual sensation such as luminance enhancement to these portions. The results also suggest that low-level image features and higher preceding cognitive context are integrated into a unified topographic representation of occluded portion in early areas.

Introduction

The contents of our visual perception are more than simple transcriptions of scenes projected on the retina: even when objects are largely occluded by neighboring objects, we can readily and effortlessly perceive each object shape by completing the occluded portion. This remarkably constructive way of visual processing of occluded objects is termed "amodal completion" (Michotte et al., 1964; Kanizsa, 1979) because the completion is mediated amodally (without any concurrent sensory representation of the completed region). The neural mechanism underlying amodal completion has been a functionally and ecologically significant topic of interest (Nakayama et al., 1990, 1995; Pessoa et al., 1998; Albright and Stoner, 2002; Kellman, 2003; Komatsu, 2006). Recent physiological and imaging studies have accumulated evidence that complete visual representations of partially occluded objects are established within visual cortex, at least in higher object-selective lateral occipital regions (Kovács et al., 1995; Kourtzi and Kanwisher, 2001; Lerner et al., 2002, 2004; Yin et al., 2002, Hulme and Zeki, 2007; Murray et al., 2004).

However, it remains unclear how and where in the brain occlusion completion is achieved. One possibility is that completion is mediated exclusively by high-level mechanisms without any influence on lower processing levels. This "higher" or "top-down" hypothesis may be supported by human fMRI studies demonstrating robust preferential activity in response even to partially occluded objects in higher object-selective regions, lateral occipital complex (LOC), but revealing little activity in earlier areas (Lerner et al., 2002, 2004). Alternatively, it is possible that an occluded portion of an object is processed or completed topographically at the early stage via bottom-up and filling-in mechanisms before reaching higher stage of object recognition

Received March 26, 2012; revised Sept. 11, 2013; accepted Sept. 17, 2013.

Author contributions: H.B., H.Y., T.H., S.-i.U., T.A., H.F., and Y.E. designed research; H.B., H.Y., T.H., S.-i.U., T.A., H.F., and Y.E. performed research; H.B., H.Y., and Y.E. analyzed data; H.B., H.Y., T.H., S.-i.U., T.A., H.F., and Y.E. wrote the paper.

This study was supported by JSPS Research Fellowship for Young Scientists (17-2088; to H.B.), the 21st Century COE Program, D-2 to Kyoto University, MEXT, Japan (H.Y. and Y.E.) and Grant-in-Aid for Scientific Research on Innovative Areas (23135517, 25135720) from the Ministry of Education, Culture, Sports, Science and Technology of Japan (H.Y.). We thank to J. Saiki, N. Goda, K. Maeda, N. Hagura, H. Takeichi, R. Kanai, H. Yamashiro, and M.L. Patten for comments on the early manuscripts; T. Kochiyama for technical comments; S. Takahashi, N. Goda, and T. Azukawa for cortical surface reconstructions and programming some analysis tools; and T. Yamamoto and A. Kondo for assistance with fMRI data collection.

The authors declare no competing financial interests.

Correspondence should be addressed to Hiroki Yamamoto, Department of Cognitive and Behavioral Science, Graduate School of Human and Environmental Studies, Kyoto University, Yoshida-Nihonmatsu-Cho, Sakyo-Ku, Kyoto City, Kyoto 606-8501, Japan. E-mail: yamamoto@cv.jinkan.kyoto-u.ac.jp.

DOI:10.1523/JNEUROSCI.1455-12.2013

 0270-6474/13/3316992-16$15.00/0

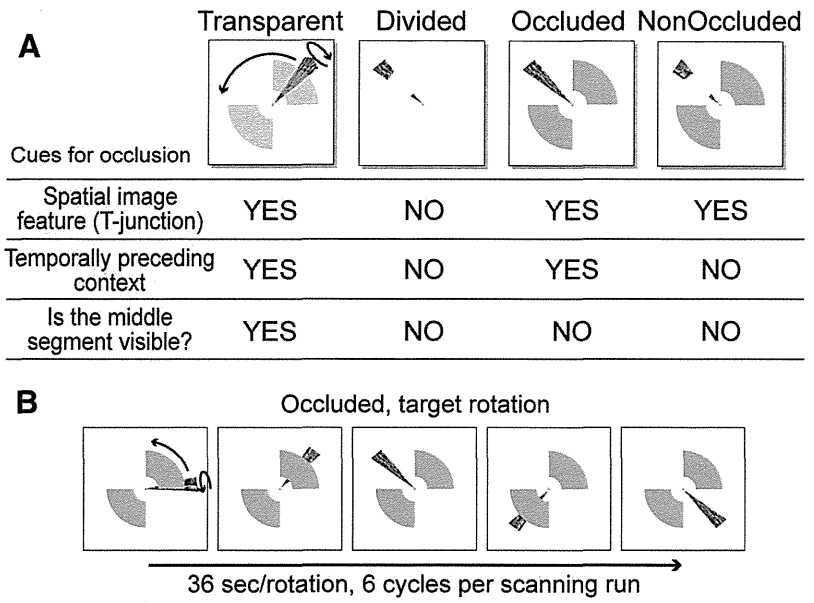

Figure 1. Experimental design and visual stimuli. ***A***, Stimuli used in the main experiment. Transparent condition: the target rotated behind two transparent occluders. fMRI activity for this stimulus is used as a baseline to assess amodal completion-related activity. Divided condition: the divided target alone rotated around the central fixation. This stimulus simulates fragmentation of visual elements due to occlusion in natural scenes. Occluded condition: the target rotated around the central fixation passing behind the occluders. In this configuration, both spatial image features, such as T-shaped junctions and temporally preceding experience with seeing, the complete appearance of the target before partial occlusion promote amodal perception. Nonoccluded condition: the divided target rotated so as to overlap two stable occluders. In this configuration, when the divided target rotated and overlapped with one of the occluders, T-shaped junctions over the occluder promote occlusion perception, although the observer who sees whole appearance of the target before overlapping knows that the target is divided, never occluded. ***B***, Schematic view of target rotation (occluded condition). Participants viewed continuous rotation of the target while fixating the central dot.

(Nakayama et al., 1995). This "bottom-up" hypothesis may be supported by physiological findings that some neurons in V1 or V2 respond to an occluded bar with crossed disparity, so that it appeared to be behind the occluder (Sugita, 1999; Bakin et al., 2000). However, the early topographic hypothesis lacks direct human neural evidence. Although a pioneering human fMRI-adaptation study reported that V1 contributes to amodal completion (Rauschenberger et al., 2006), it could be argued that the observed V1 adaptation may not reveal the reconstructed representation of the occluded portion, and instead may simply reflect adaptation to low-level image features, such as T-shaped junctions at occluding borders. To resolve these disparate accounts is important to understand how the visual system reconstructs coherent percepts from fragmentary and incomplete retinal inputs.

Here, we investigated the topographic representation hypothesis in human early visual cortex. By measuring fMRI activity within the precisely defined cortical regions corresponding to the occluded portion of an object, we provide clear evidence that human early visual areas, V1 and V2, indeed represent the occluded portion as if it were pictorially completed. The observed completion-related responses cannot be simply explained by attentional boosts of fMRI responses. Furthermore, we find that the early topographic representation of occlusion is modulated by prior knowledge of the appearance of the complete object seen before partial occlusion.

Materials and Methods

Participants

Eight healthy adults (two females, one left-handed, 31-years-old on average) with normal or corrected-to-normal vision participated in the main experiments. Eight adults participated in an additional attention control experiment (all males, one-left-handed, 28 years old on average). Three males participated in both experiments. All participants provided oral and written informed consent. All participants had experience in psychophysical experiments and were well trained to sustain eye fixation. The Ethics Committees of the Graduate School of Medicine and that of Human and Environmental Studies, Kyoto University, approved the experimental procedures in advance.

Visual stimuli and experimental design

Visual stimuli were generated on a PC using a publicly available OpenGL-compatible Visualization Toolkit (VTK) C++ library (Kitware). The stimuli were presented via a gamma-corrected (Ban and Yamamoto, 2013) digital-light-processing type projector (U2-1130, PLUS Vision) and back-projected onto a translucent screen. Participants viewed the screen through a first surface mirror tilted 45° and positioned in front of the participant's forehead.

The stimuli consisted of a continuously rotating volumetric triangular wedge (target) and two stable occluders (Fig. 1). The target wedge spanned 20° in polar angle and extended 12.5° of visual eccentricity from a point of central fixation. On the target, a continuous brick-wall texture was mapped to enhance pictorial depth perception and local luminance changes accompanying the target rotation. The occluders were uniform gray and covered 4.2–8.3° in eccentricity in the upper-right and lower-left visual field quadrants and were stable in shape and size throughout a scanning run.

In the main experiments, we manipulated the spatial and temporal configurations of the stimuli using the following four experimental conditions: transparent, divided, occluded, and nonoccluded (Fig. 1*A*). In the transparent condition, the occluders were transparently rendered using OpenGL opacity function (set to 0.5) and the target rotation behind the transparent occluders was visible. In the divided condition, the occluders were removed from display and the target was divided by removing the middle segment of the target that was to be occluded; observers viewed the divided target rotation alone. Here, this stimulus configuration may be, at a glance, perceived as the whole target rotated behind a gray (same color with the background) annulus occluder. However, the target stimulus is actually a volumetric triangular (3D) wedge projected on a 2D screen. Therefore, when it is divided and rotated along its own axis, visible triangular edges at the middle segment prevented the target from being perceived as if it is occluded by the invisible apparent occluder. All the participants actually reported that the target was divided without any occlusion percept when the stimulus was presented outside the scanner in advance of the main experiment. In the occluded condition, the target rotated behind two stable opaque occluders and the middle segment of the target was invisible when the target came to the upper-right or lower-left visual quadrant. In the nonoccluded condition, the divided target (the part that would be masked by the occluder has been removed) rotated and two stable opaque occluders were located in the upper-right and lower-left visual field quadrants. In this condition, although the target was divided, the stimulus spatial configuration was the same with occluded condition when the target passed through one of the occluders, whereas an observer seeing the sequence of target rotation knew that the target was divided. This configuration was used to test whether preceding cognitive context (observer's knowledge about the appearance of the target acquired

before the target came to overlap with the occluders) could be reflected in occlusion completion-related fMRI responses.

In all stimulus conditions, the target began to emerge from slightly below the right horizontal visual meridian and rotated smoothly around a central fixation point in a counterclockwise fashion at a rate of 10 deg/s (Fig. 1*B*). To enhance the impression of occlusion by pictorial and motion cues, we also put the target rotation around its own axis at 120 deg/s (see arrows in Fig. 1*B*). The target rotation around the central fixation (36 s/rotation) was continuously repeated 6 times in an fMRI scanning run. An fMRI scanning run thus lasted 216 s, plus a 10 s adaptation period at the beginning of each scan to prevent startup magnetization transients.

Participants viewed the target rotations sustaining eye fixation on the central fixation point. Control of participants' attention and blocking of effects of eye movement were also of crucial importance for the present study. We therefore imposed an attention-demanding task related to the central fixation point. Specifically, the color of the fixation point changed randomly (at 1 s intervals, 500 ms duration) to red, green, blue, or yellow, and then turned back to pale blue (default color). We instructed participants to press an optical switch when the color of the fixation point turned red. Image data with <80% correct responses to the fixation task were discarded.

To discriminate effects of attentional boosts on fMRI activity from the amodal completion-related responses, we further conducted an additional control experiment with manipulating the central fixation task difficulty. In this control experiment, the color of the central fixation changed more frequently (at every 500 ms, 200 ms duration) and participants were asked to concentrate on the same color detection task through all scans. The ratio of correct responses for this experiment was 60–80% and all the data were used.

These and the other stimulus parameters such as size, luminance, and speed of the target rotation were set to optimize the perceptual salience of amodal completion on participants' reports outside the scanner, and for clear and reliable determination of cortical retinotopic representation. Further, the luminance contrast of the occluders from gray background was set relatively high (120 cd/m^2 for the uniform gray background, 194 cd/m^2 for the occluders) as to avoid the Troxler effect (Friedman et al., 1999; Von der Heydt et al., 2003; when steady fixation is maintained, the contrast of an object in the peripheral visual field gradually decreases, and the object finally becomes invisible). The continuous target rotation sweeping the entire visual field repeatedly also minimizes such effects.

The "amodal" nature of occlusion perception, which is accompanied by no concurrent sensory representation such as luminance enhancement of the occluded portion, makes it difficult to measure perceptual performance quantitatively. However, through questionnaire and actual stimulus demonstrations on computer displays outside the scanner in advance of the scanning session, all participants reported occlusion percepts for occluded and not for divided condition. In nonoccluded condition, when the target overlapped with the occluders, all participants reported occlusion-like percepts promoted by spatial image features, such as T-shaped junctions at the occluding borders, but nonetheless reported that they knew the target was divided, and not occluded.

Imaging data acquisitions

Participants were scanned on 3.0 tesla Siemens MAGNETOM Trio Scanner equipped with an eight-channel phase-array head coil (Siemens) at the Graduate School of Medicine, Kyoto University, Japan. Blood oxygenation level-dependent (BOLD) contrast was obtained with a gradient-echo echo-planner imaging (EPI) sequence (TR 2000 ms, TE 30 ms, flip angle 90°, matrix size 64 × 64, voxel size 3 × 3 × 3 mm^3 without gap). The scanned volume included 24 slices nearly perpendicular to the calcarine sulcus. The onset of stimulus presentation and fMRI scanning were synchronized using a custom-made triggering system. Data acquisitions were repeated at least four times for each stimulus condition in a day. T1-weighted 3D high-resolution (voxel size 0.94 × 0.94 × 1.0 mm^3, 208 axial slices) anatomical images were also acquired for each participant to allow accurate spatial coregistration between functional and anatomical image data, cortical gray/white matter segmentation using mrGray software (Teo et al., 1997), and cortical surface reconstruction (Yamamoto et al., 2008, 2012).

Reconstruction of the cortical surface

The cortical surfaces of the individual participants were reconstructed from the structural T1-weighted image volumes. The detailed procedures are described previously (Yamamoto et al., 2008, 2012). Briefly, we generated the surface lying approximately in the middle of the gray matter using a method that was a hybrid of volume segmentation (Drury et al., 1999) and surface deformation (Dale and Sereno, 1993) techniques. First, the voxels that belonged to the cortical gray matter were segmented from the rest of the volume using mrGray software. mrGray enabled us to identify the white matter, CSF, and three layers of gray matter semiautomatically. The segmented gray matter was ~3 mm thick and they were classified the first, second, and third layers from the gray-white matter boundary. The segmented volume was then smoothed using a 3D Gaussian filter to minimize any nonbiological irregularities. Next, a surface representation was created for the gray-white matter boundary. At this point, we did not create the surface for the middle of the gray matter to minimize topological defects, such as bridges between cortical sulci. We then computed a concrete mean voxel value for the first gray matter layer in the smoothed segmented volume and applied the marching cube algorithm (Lorensen and Cline, 1987), which extracted an isosurface tessellated with ~300,000 triangles. The number of triangles was then reduced to 200,000 using the decimation algorithm (Shroeder et al., 1992). Finally, the triangulated surface was deformed such that it lay in the middle of the gray matter by relaxing it against the smoothed segmented volume. We used the deformable template algorithm (Dale and Sereno, 1993) for deformation. Finally, the resultant surface was visually inspected for positional accuracy and topological errors by overlapping it with the original structural MR volume. An additional method used to detect topological defects was extensive smoothing of the surface, which highlighted the surface defects as sharp edges. If the surface was inaccurate or had severe defects, corrections were made in mrGray manually and the subsequent procedures were repeated. We also created inflated, that is, hyper-smoothed versions of the reconstructed surfaces. We used an inflation algorithm that was essentially similar to that proposed by Fischl et al. (1999). Each participant's functional data were coregistered into individual reconstructed surface space. Reconstructed cortical surfaces were used to visualize cortical activity, to identify retinotopic visual areas, and to sample functional voxels in the target regions of interest.

fMRI data analyses.

Preprocessing. For all fMRI data, the first five volumes were discarded to prevent startup magnetization transients. All data underwent slice-timing correction and 3D motion correction (Woods et al., 1998). Slow drifts in signal intensity were removed by a classical decomposition technique as all data contained periodic responses. Then, the imaging data were coregistered to the anatomical volume. All data were analyzed in these individual anatomy spaces. No further spatial/temporal smoothing and spatial normalization (e.g., Talairach transformation) were applied.

Identifying retinotopic visual areas. Before conducting the main experiments, we performed retinotopy localizer scans (at least four scans for each of polar and eccentricity maps) and identified 12 visual areas, V1d, V1v, V2d, V2v, V3d, V3v, V3A, V3B, V4v, V7, LO (lateral occipital region), and MT+, following the standard phase-encoded analysis technique (Engel et al., 1994; Sereno et al., 1995; DeYoe et al., 1996) for each participant (Fig. 2). We used luminance and chromaticity flickering (10 Hz) checkerboard patterns for these retinotopy scans. The details were described previously (Yamamoto et al., 2008, 2012). The polar angle map allowed us to identify the borders of V1d(v)/V2d(v), V2d(v)/V3d(v), V3d/V3A (Tootell et al., 1997), and V3A/V7 as reversals in the polar angle and field-sign map. Eccentricity map was also used to identify V3A, V3B, and V7 borders as the foveal representations of these areas were displaced superiorly with the confluent foveal representation of areas V1, V2, and V3 (for a review, see Wandell et al., 2005, 2007). We identified V3B (Smith et al., 1998) so that it was located just anterior to V3d and its foveal representation was just adjacent to the V3A foveal representation. We identified MT+ as the region within the dorsal posterior limb of the inferior temporal sulcus, which had a crude eccentricity map with predominantly foveal representation superiorly and peripheral representation inferiorly (Huk et al., 2002). We confirmed that this region mostly

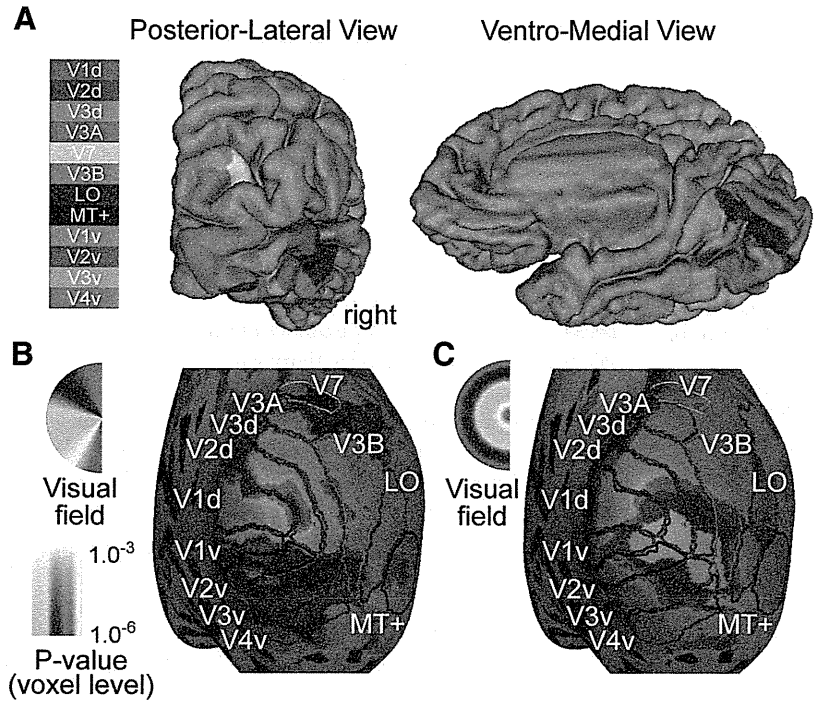

Figure 2. Identified retinotopic visual areas. Twelve retinotopic regions of interest. ***A***, Locations of the visual areas V1, V2, V3, V4v, V3A, V3B, V7, LO, and MT+ in one subject's right hemisphere from posterior lateral view (left) and ventromedial view (right). The icon to the left of the panel indicates the relationship between color and visual area. Borders of the areas were determined from the polar-angular (***B***) and eccentricity (***C***) visual field representations measured by separated phase-encoded retinotopic mapping experiments. The color overlay on the inflated cortex indicates the preferred stimulus angle or eccentricity at each cortical point, and the colored lines indicate each area's border. The icons to the left of each panel indicate the relationship between color and visual field position.

overlapped with the middle temporal region, and exhibited a strong response to motion stimuli. We refer to the large fan-shaped region between areas V3B and MT+ as LO (Malach et al., 1995), which had a relatively clear polar and eccentricity representations (Levy et al., 2001; Larsson and Heeger, 2006). There is an enduring dispute regarding subdivision of the ventral occipital cortex anterior to V3v (Wandell et al., 2005, 2007). Here, we identified an area, V4v, after Hadjikhani et al. (1998) stressing consistency not in the angle but in the eccentricity map in our data (Yamamoto et al., 2012). V4v in this study roughly corresponded to the posterior half of hV4 (Zeki et al., 1991; Bartels and Zeki, 2000; Brewer et al., 2005). Note that we also analyzed data of some participants by reidentifying these regions as hV4 and VO1/VO2 using different criteria (Brewer et al., 2005), but we could not find any differences of the results in the present study.

Identifying regions of interest. Then, we further localized the cortical subregions in each retinotopic area (V1, V2, V3, and V3A) that corresponded to the locations of the occluders presented in the subsequent main experiments (see Fig. 4*A*, bottom left). The localized regions were used as regions of interest (ROIs) for the analyses of the main experiments. These ROIs were identified in separate block-design scans for each participant and each scanning day (two runs per participant and per day) by presenting flickering checkerboards in the same locations of two occluders used in the main experiment alternating with the compensating checkerboard pattern. To identify the occluder regions, we applied the standard GLM analysis (occluder position vs the compensating pattern) on the data and extracted voxels from each visual area that showed responses at $p < 0.001$ (uncorrected) for the checkerboard pattern corresponded to the occluder positions. We also localized foveal and peripheral regions that were external to the occluders for each early visual area. For V3A, we could only roughly localize two subregions, corresponding to the occluders and the external regions because V3A had a hemivisual field representation and retinotopy was not as clear as that observed in V1–V3 (Fig. 2*B*,*C*; see Fig. 4*A*, bottom left).

Phase-encoded analysis to evaluate cortical retinotopic activity corresponding to the occluded portion. Target rotation around the central fixation point caused periodic shifts of neural activity in the early visual areas; because their neurons have limited receptive fields whose centers are organized to form a continuous mapping between the cortical surface and the visual field, a portion of the early visual cortex responded periodically when the target swept across the corresponding visual field location (Wandell et al., 2007). We investigated whether we could observe this periodical shift of activity even when the target stimulus rotation was partly occluded. To evaluate retinotopic periodic responses, the data were analyzed using a Fourier transformation-based method, well documented in the standard retinotopy studies (Engel et al., 1994; Sereno et al., 1995; DeYoe et al., 1996). First, a Discrete Fourier transformation was computed for the time series of each voxel after converting the raw signals to percentage signal changes. Then, statistical testing to estimate the significance of correlation of BOLD signal at the stimulus frequency (1/36 Hz) was performed by comparing the squared amplitude at the stimulus frequency with the sum of squared amplitudes at the other frequencies, which yielded an *F*-ratio. The *F*-ratio was converted to a *P* value considering degrees of freedom of the signals (number of time points). In mapping retinotopic responses on the cortical surface, the polar angle phase of each significantly activated voxel was displayed using a continuous color scale. Here, a voxel-level Fourier *F*-statistic value, $F_{(2,105)} > 7.38$ and $p < 0.001$ (uncorrected), was used as a criteria of significance for all Fourier-based analysis (e.g., mapping activity on the cortical surface) if there is no further information.

Mapping fMRI responses on reconstructed cortical surface. We visualized imaging data by on the reconstructed cortical surfaces generated following the procedures described above. The surface representation was created by sampling the voxel responses at each node of the surface mesh within a radius of 4 mm and averaging them. The representation was color-coded by assigning different colors to different response phases, and by altering the saturation of colors such that each color increased saturation corresponded to a statistical significant level.

Subdivision of ROIs and detailed voxel-based analysis. To evaluate the periodic fMRI responses quantitatively and to investigate the spatial specificity of the periodic responses, we further performed detailed voxel-based analyses. To this end, each of the retinotopic ROIs (subregions in V1–V3 that corresponded to the occluder retinotopic positions) were further divided into three subregions along cortical visual-field polar angle or eccentricity representation for each participant. fMRI responses were separately resampled within these subregions and compared. Visual-field polar angle representations were determined based on cortical activity evoked by the transparent stimulus (Fig. 1*A*). Eccentricity representations were determined by an expanding ring stimulus used in the standard retinotopic experiments. fMRI voxel responses were resampled at each node of these sub-ROIs' meshes within a radius of 2.5 mm. Note that, in all the voxel-based detailed analyses, all voxels located along the border of each ROI (~2 mm radius from the borders) were carefully removed in advance because it is possible that these voxels contain BOLD responses from neighboring regions where target rotation is completely visible. We thus compared neural activity only within the strictly limited regions of predefined ROIs that retinotopically represent regions covered by the occluders. The number of voxels survived in this preprocessing were 21.94 ± 9.03 (mean and SD) in V1 sub-ROI, 15.06 ±

7.03 in V2, and 13.25 ± 3.45 in V3. For some sub-ROIs of a few participants, we omitted the data from the detailed voxel analyses since we could not segregate the ROIs into three subregions with precision. Thus, statistical tests in the detailed sub-ROI analyses were performed with $n = 6$ in V1, V2, and V3, whereas the other tests were performed with $n = 8$ in all ROIs.

Even after these retinotopy-based restrictions of voxels, it would be difficult to completely exclude the periodic responses from the outer regions to the occluder ROIs due to BOLD spreads. To rule out this confound more strictly, we further restricted the sub-ROIs by excluding any voxels that showed significant responses to the divided stimulus in the same scanning session. Specifically, after defining the occluder ROIs, we extracted all voxels that showed $F_{(2,105)} > 3.08$ and $p < 0.05$ (uncorrected) for the divided condition in some additional analyses.

Comparisons of voxel-based periodic activities among conditions. To compare periodic response magnitudes evoked by the visible and invisible target rotations, we calculated a relative periodicity index following the same procedures of Fourier F test described above. Specifically, we first computed voxel-by-voxel periodicity for each stimulus condition, by dividing the squared amplitude at the stimulus frequency (1/36 Hz) with the sum of squared amplitudes at the other frequencies. Here, the value indicates how strongly a voxel responds to the invisible (occluded or divided) target. Then, to directly compare periodic powers across conditions, the calculated periodicity of each voxel for the occluded condition was divided by the corresponding voxel periodicity for the divided or nonoccluded condition. These values were averaged across voxels, yielding a relative periodicity index in each ROI.

Completion index. We calculated completion index for each participant to directly compare the similarity of neural activity evoked by the invisible target rotation with that evoked by visible rotation. The completion index was defined as

$$Completion\_Index = \frac{1}{n} \times \sum_{i=1}^{n} \left(\frac{\vec{a}_i \cdot \vec{b}_i}{|\vec{b}_i|} \times \frac{1}{|\vec{b}_i|} \right),$$

where n is the number of voxels within a ROI, $\vec{a}$ is a vector consisting of the response amplitude and phase angle of a voxel for the occluded (or divided) stimulus ($\vec{b}$ = amplitude, phase), and $\vec{b}$ is a vector for the corresponding voxel response to the transparent stimulus. This index is 0 when there is no response to the invisible target rotation, negative when the responses to the invisible rotation are opposite to the visible responses, positive (usually <1) when the responses for the invisible rotation is similar with the visible rotation, and equal to 1 when the invisible target evoked exactly the same response as the visible target did. In calculations, data from the two hemispheres were averaged, because no significant difference was observed between responses in the retinotopic regions corresponding to lower-left and upper-right visual field quadrants. Unlike the periodicity analysis described above, which took into account only powers of periodicity at the target frequency (1/36 Hz) and did not consider response phases, this correlation-like analysis considered both phase and periodic power components simultaneously. This indexing analysis thus involves a more conservative approach to investigating completion-related activity.

Results

Experimental design

The target visual stimulus was a volumetric triangular wedge that continuously rotated around a central fixation point (36 s per rotation, 6 rotations per scanning session) while rotating around its own axis (Fig. 1*B*). In the scanner, participants viewed the target rotation while maintaining fixation on the center of the screen and performing a color detection task on the fixation point. Rotation of the target around the central fixation causes periodic shifts of neural activity as to sweep the retinotopic visual cortex as shown in standard retinotopic studies (Engel et al., 1994; Sereno et al., 1995; DeYoe et al., 1996). We used this property of periodic activity to access amodal completion-related neural responses. That is, we explored how the periodic activity corresponding to the target rotation was modulated when perception of the target was changed by systematically manipulating the target appearance and/or its surrounding spatial and temporal contexts leading to modal or amodal completion. We reasoned that visual areas whose activity reflects the topographic interpolation of amodal completion, if they exist, should exhibit robust periodic responses even to the occluded rotation in the absence of direct sensory input.

fMRI responses to a visible object in retinotopic visual areas

We first measured cortical activity with completely visible target rotation as a baseline for each participant to evaluate amodal completion-related activity for subsequent stimuli. Here, to match stimulus configurations, such as edges with the stimuli described below, we additionally presented static transparent occluders in the upper-right and lower-left visual field quadrants (Fig. 1*A*, transparent condition). This visible target rotation caused reliable periodic shifts in neural responses in overall visual eccentricity spanning the rotating target.

Here, it is possible that the transparency of the occluders may cause systematic shifts in response phases (delays) in retinotopic areas that result in inadequate evaluation of amodal completion-related activity. To rule out the possibility in advance, we compared phase-encoded responses evoked by transparent stimulus with those evoked by target rotation alone. As shown in Figure 3, the two stimuli yielded similar response patterns in early retinotopic visual areas without any response biases due to transparency. We therefore conclude that transparency of the occluders did not affect the following analyses.

Next, we explored how the observed retinotopic activity was modulated when the target was divided into two separate portions by removing the middle segment (Fig. 1*A*, divided condition), simulating virtual fragmentations and separations of an object that are often occur in natural scenes due to occlusion. In all participants, division of the target caused division of activation pattern on the cortical surface in V1 and V2 (Fig. 4*A*, top, left and right). The missing region of fMRI activity was confined to retinotopic subregions corresponding to the divided segment, which had been separately identified by additional localizer scans for each participant (Fig. 4*A*, bottom left; see Materials and Methods).

The separation of cortical representations of the separated visual elements has the following important implications for object representation in early retinotopic areas. First, in these areas, an object is represented by neurons whose receptive fields are too small to capture both of the divided visual elements. Second, although the separated visual elements undergoing synchronous motion induced a percept of them as a single virtual wedge-like object, the representation corresponding to such perceptual integration and completing the missing region were not used in these areas (but see Meng et al., 2005). Third, in our experimental conditions, in which participants performed a color detection task on the central fixation point through a scanning session, the representation did not include attentional (Somers et al., 1999; Sasaki et al., 2001) or imagery (Slotnick et al., 2005) effects radially spreading along the divided segments that could result in neural completion of the missing portion. Together, these findings suggest that early visual areas generally respond to only visible portions of objects based on direct sensory inputs from retina to cortex.

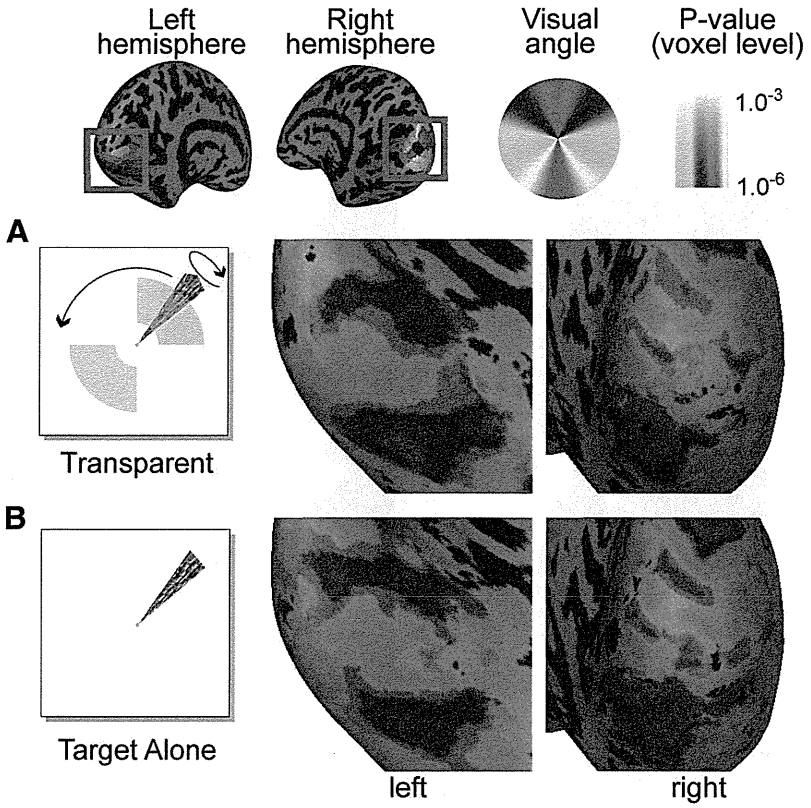

Figure 3. Representative cortical activity in response to transparent and real target rotations. Response phase angles of significantly (Fourier F test, $p < 0.001$, voxel level) activated voxels projected on participant's inflated occipital cortex. ***A***, Phase-encoded responses for target rotation behind transparent occluders (transparent condition). ***B***, Phase-encoded responses for target rotation alone.

Topographic fMRI responses to an occluded object

Then, what neural activity is observed in retinotopic early visual areas when the target rotation is partially occluded by an opaque occluder? We measured cortical activity while participants viewed the partially occluded target rotation (Fig. 1*A*, occluded condition). Note that, in this configuration, the target rotation is completely divided, as in the divided condition, and that the middle segment of the target is completely invisible while the target passes behind the occluders. Thus, if early visual areas truly represent only visible portions of an object, the pattern of cortical activation by this occluded rotation should again be divided, and no periodic neural response should be observed within the retinotopic subregions representing the occluders.

However, we found clear periodic shifts in activity corresponding to the occluded and invisible target rotation, as if the gap between the visible portions of the target had been bridged despite lack of direct sensory input to these regions. Although the responses were not as strong compared as those evoked by the transparent stimulus, V1 and V2 exhibited robust activation even for the occluded portion (Fig. 4*A*, bottom right; *B*, averaged time courses from three subportions in V1, V2, and V3). Because similar completion-like activity was not observed or weaker (Fig. 4*A*, top) in the divided condition, the observed periodic activity cannot be simply explained by fMRI signal leakage from external (foveal/peripheral) regions of the occluders, where rotation was completely visible. Furthermore, because the occluders were presented stable in specific locations during a scanning run and our analysis is targeting periodic activity (signal power at 1/36 Hz included in the time series), the observed periodic activity in the occluded condition cannot be explained as an effect of the opaque occluders alone. The observed activity thus may reflect topographic activity to the invisible part of the target stimulus; geometric relations and interactions between the target and occluders may allow visible portions of an object to be connected under occlusion and may promote completion-related neural responses.

We need to note, however, that those simple analyses cannot completely rule out the alternative possibilities. We generated the cortical response maps by sampling voxels within relatively large space (4 mm radius from each cortical surface node). Therefore, there is no evidence that responses within the occluder ROIs were really free from the response confounds from visible regions. In addition, our phase-encoded experiment paradigm might work so as to bias the averaged time courses due to the effect of negative BOLD signals, etc. Specifically, it might be possible that the divided condition may show some opposite response profile (in Fourier phase domain) compared with the transparent condition. In that case, responses of the occluded condition would become relatively larger than the divided even without any actual completion-related activities. Then, we may mistakenly conclude that seemingly larger activity for the occluded condition would be related to occlusion completion. To rule out these possibilities and to confirm the topographic completion-related responses, we conducted more conservative and detailed analyses. In the following analyses, voxels located along the border of each ROI were carefully omitted. Further, the analysis was limited to voxels that were significantly activated by the ROI localizer (voxel-wise t test; $p < 0.001$, uncorrected) and that exhibited significant retinotopic responses (Fourier F test; $F_{(2,105)} > 7.38$, $p < 0.001$, voxel level) for the transparent stimulus (see Materials and Methods).

First, to test whether the occluded target rotation actually caused periodic responses to complete the invisible portion, we explored the relationship of voxel-by-voxel Fourier powers and phases between the transparent and occluded/divided conditions in V1–V3 subregions that retinotopically represented the occluder positions. If the occluded condition actually caused completion-related responses, these response phase profiles in ROIs would be similar with those of the transparent condition. The results were scatter-plotted in Figure 5. In these plots, larger dots indicate larger periodic powers (and thus smaller p value in Fourier F-statistics). By visual inspection, we found clear correlations of response phases between the occluded and transparent conditions. Furthermore, we could confirm that no voxel with opposite phase and strong periodicity was included in the occluded condition (Fig. 5*A*). Therefore, we can conclude that the occluded condition actually caused positive completion-like activity to the invisible target rotation. Note that we also found some voxels that had strong periodicities corresponded to the invisible target rotation even for the divided condition. However,

the total number of these periodic voxels was smaller than that of the occluded condition (Fig. 5*B*). The observed strong activity even in the divided condition would be probably due to inevitable BOLD spreads from outer regions. We conducted further detailed analyses to exclude these effects later.

To quantitatively evaluate these periodic responses, we directly compared powers of periodic responses (periodicity) evoked by the occluded stimulus with those by the divided, focusing on the responses within the predefined ROIs in V1–V3 representing the occluded portions (Fig. 6; see Materials and Methods). Here, higher periodicity of a voxel indicates stronger response at the stimulus frequency (1/36 Hz) corresponding to invisible target rotation. Calculated relative periodicities (periodicities of the occluded condition was divided by that of the divided) revealed that V1–V3 exhibited significantly higher completion-related periodic responses for the occluded stimuli (paired t tests to access whether the relative periodicity is >1, $t_{(7)} = 2.84$, $p = 0.014$ in V1, $t_{(7)} = 5.65$, $p = 0.00039$ in V2, $t_{(7)} = 3.63$, $p = 0.0042$ in V3. All ROIs were significant at $p < 0.05$ level after adjusting p values for multiple-comparisons using Bonferroni correction method).

It might be argued that the observed completion-like activity is not derived from the resultant neural representation of the occluded region, and instead simply reflects responses to edges generated at the boundaries of occlusion. To test this possibility, we examined the temporal and spatial specificity of the completion-like activity. We resampled cortical responses separately along visual field polar or eccentricity representations within three subregions in each ROI for each participant. If the observed responses reflected only the occluding edges, the periodic responses would not be observed in the middle position of each ROI. In contrast, if the responses truly reflected the neural representation of the occluded portion, the periodic responses separately resampled along visual polar/eccentricity representations would exhibit no bias in visual field location.

First, we plotted voxel time courses for the occluded stimulus resampled separately along polar visual angles. As shown in Figure 7*A*, responses were periodically shifted even after the target had completely entered the region of occlusion, indicating that the neural representation of the invisible rotation is updated from moment to moment without direct sensory

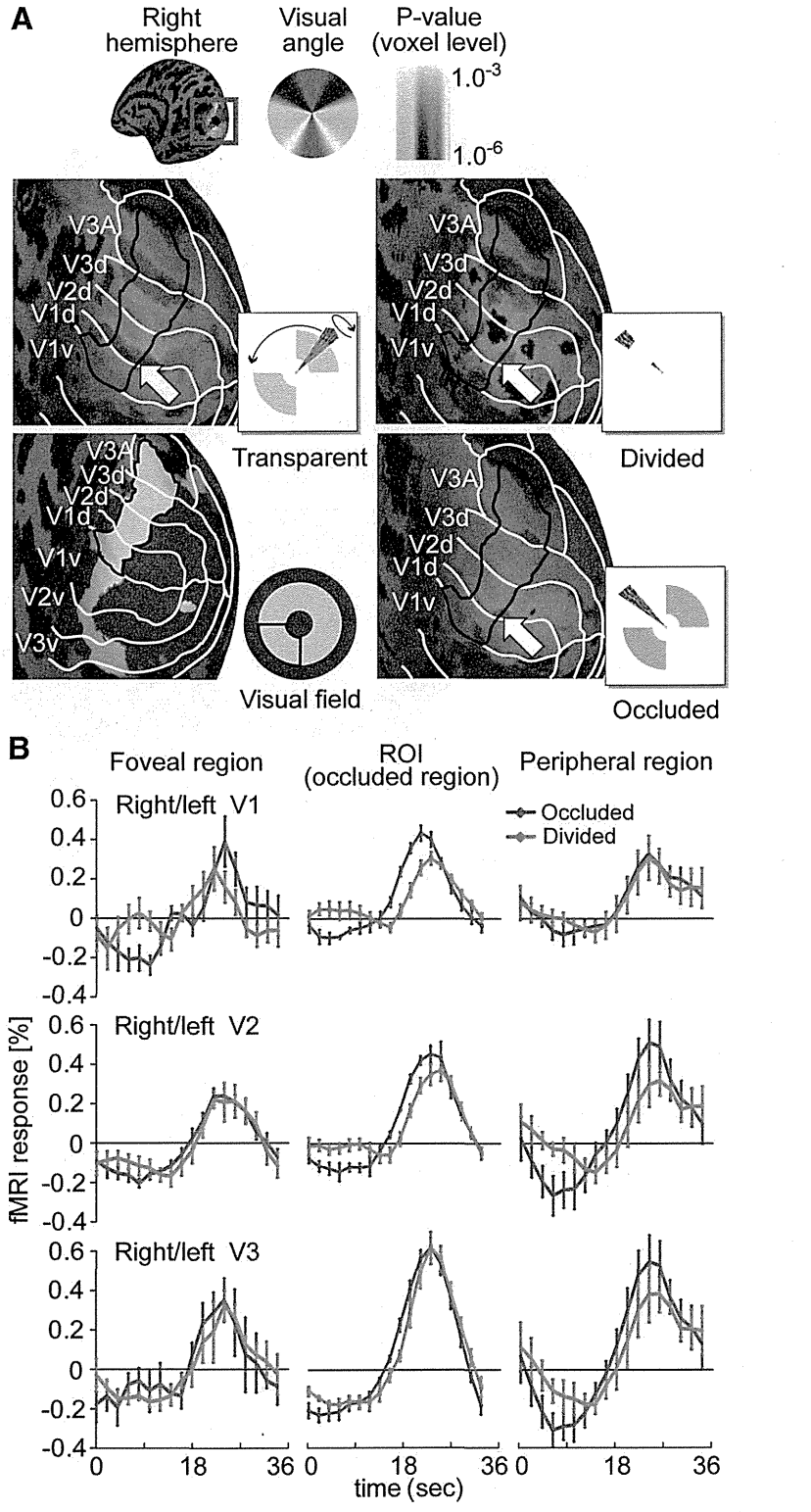

Figure 4. *Representative cortical responses and fMRI time series for Occluded and Divided stimuli.* ***A****, Top left and right, and bottom right panels,* Cortical responses projected on representative right inflated cortical surfaces (voxels with $p < 0.001$ in voxelwise Fourier F test were mapped). Colors represent the corresponding visual field locations as shown the icon above. Color saturations represent statistical p values. The black solid lines indicate retinotopic subregions representing the lower-left occluder. The white lines indicate retinotopic visual area borders. Bottom, left, Cortical activity in response to the checkerboard stimulus used for localizing the cortical subregions representing the upper-right and lower-left occluders. ***B****,* Averaged fMRI signal time courses evoked by the occluded and divided stimuli in V1, V2, and V3. Left/right columns show the averaged voxel time courses sampled from the foveal/peripheral regions of the retinotopic subregion corresponding to the occluded portion. Middle column show the averaged voxel time courses corresponding to the occluded portion. Here, the response phases of voxels were aligned to 16 s after the first stimulus presentation by linear interpolating and shifting the time courses voxel-by-voxel based on the response phases evoked by the transparent stimulus. Error bars, SE.

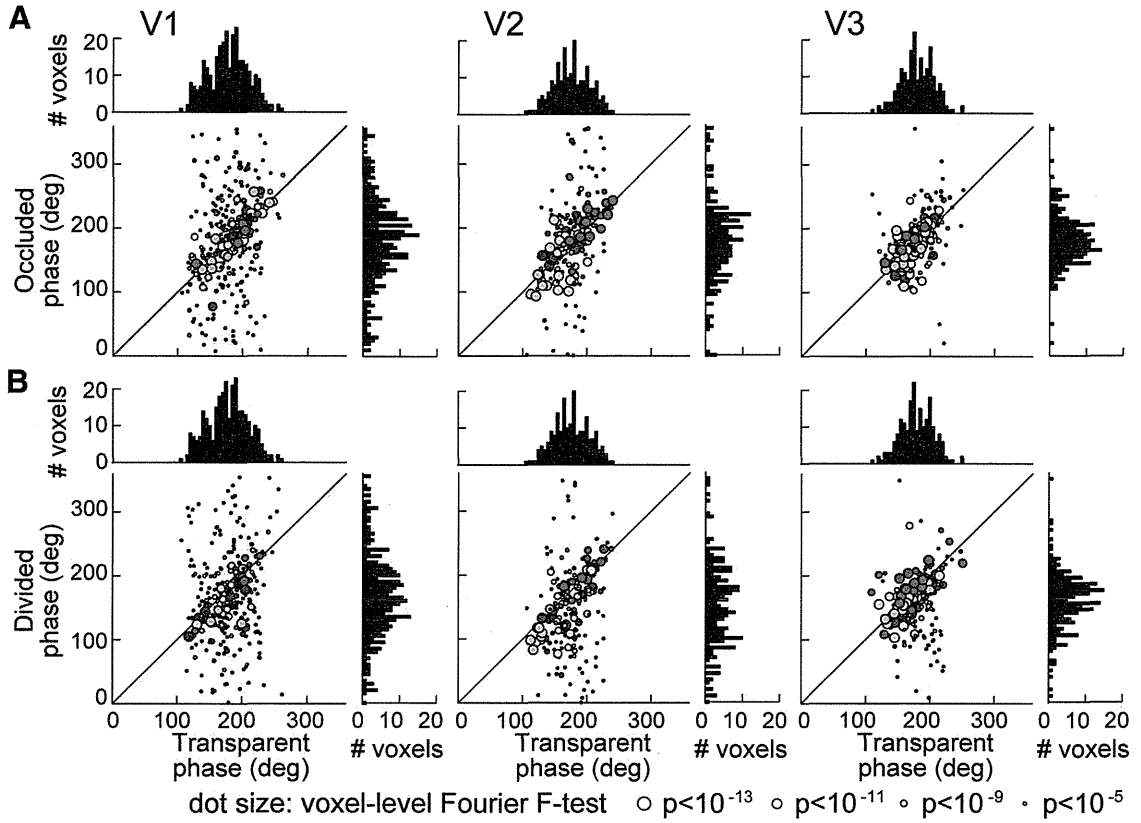

Figure 5. Relationship of response phases between the transparent and occluded/divided conditions. ***A***, Voxelwise phase scatter plots, transparent versus occluded. Each dot represents individual voxel. Each color represents single participant. Dot sizes represent magnitudes of Fourier *F*-statistics (and the corresponding statistical *p* values). Larger dot indicates that the voxel contains higher-power at the target rotation frequency (1/36 Hz) compared with the sum of the powers at the other frequencies. Here, for legibility, the response phases of voxels were aligned so that the center of response phases of each ROI comes to 180° by voxel-by-voxel linear shifting based on the response phases evoked by the transparent stimulus for each participant. ***B***, Voxelwise phase scatter plots, trasnparent versus divided.

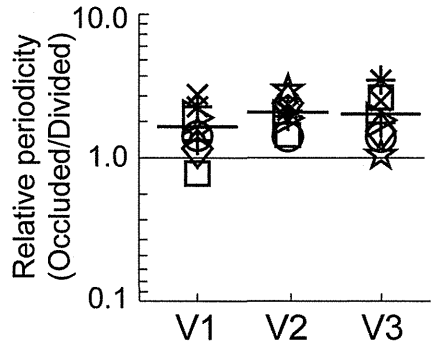

Figure 6. Relative periodicity (occluded/divided) in V1–V3 ROIs. Relative periodicity plots in V1, V2, and V3. Each shape represents a single participant. Horizontal bars represent mean values.

input. Next, we compared relative periodicities resampled along visual polar angles. As shown in Figure 7*B*, we found no bias in visual position; one-way (visual polar angles, six locations) repeated-measures ANOVA revealed no main effect of visual location ($F_{(5,30)} = 0.75$, $p = 0.59$ in V1; $F_{(5,35)} = 0.62$, $p = 0.68$ in V2; and $F_{(5,35)} = 0.43$, $p = 0.82$ in V3). Thus, the observed responses are not derived simply from occluding edges generated when the target enters the occluder. Further, we compared relative periodicities resampled along visual eccentricity. As shown in Figure 7*C*, the periodic responses were not limited to nearby regions of foveal/peripheral edges of the occluders (one-way repeated-measures ANOVA revealed no main effect of visual field location; $F_{(5,30)} = 0.07$, $p = 0.99$ in V1; $F_{(5,35)} = 1.07$, $p = 0.40$ in V2; $F_{(5,35)} = 0.40$, $p = 0.85$ in V3). In sum, these comparisons of periodic responses over retinotopic subregions revealed that the observed activity reflects the neural completion responses.

Comparison of neural responses to amodal and real objects

We then tried to quantitatively estimate how robust the representation of an occluded object was, compared with that of its real counterpart. To this end, we calculated a completion index for each ROI (see Materials and Methods). Briefly, the index was defined as the mean of components of voxel response amplitudes evoked by an amodal surface with zero phase (delay) lags relative to the response from a real surface. If the index is 1, neural activity for the amodal rotation is completely identical to that for the visible target rotation, whereas an index of 0 indicates no completion-related response. Here, baseline neural activity of a real surface was determined separately for each participant as activity evoked by the transparent stimulus. Completion indices for the divided stimulus were also calculated for comparison. Note that this analysis can evaluate completion-related activity more conservatively than the periodicity analysis described above (Figs. 6, 7), because not only the power of periodic response but also the response phase (delay) of each voxel is taken into account. Specifically, when we only focus on periodicities of voxel responses (1/36 Hz), both positive and negative signals would equally contribute to boost periodic powers in ROIs, although

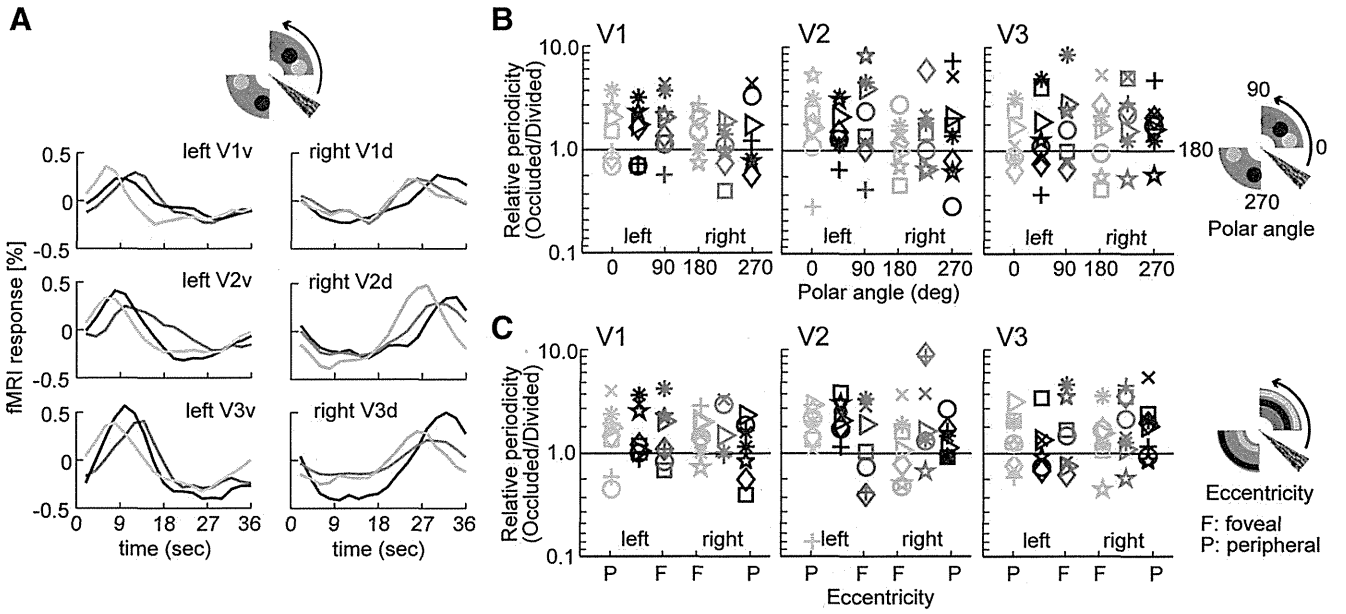

Figure 7. Temporal and spatial specificity of completion-related responses. Voxel-by-voxel responses were resampled along visual field polar angle or eccentricity representation. ***A***, fMRI voxel time courses evoked by the occluded stimulus sampled and averaged separately from three subregions of each ROI along the cortical visual polar angle representations. Each color represents the corresponding visual field location. ***B***, Comparison of relative periodic responses (occluded/divided) along polar angle representation. Each shape represents a single participant. Each color represents a single retinotopic position as shown in the right icon. ***C***, Comparison of relative periodic responses (occluded/divided) along visual eccentricity representation.

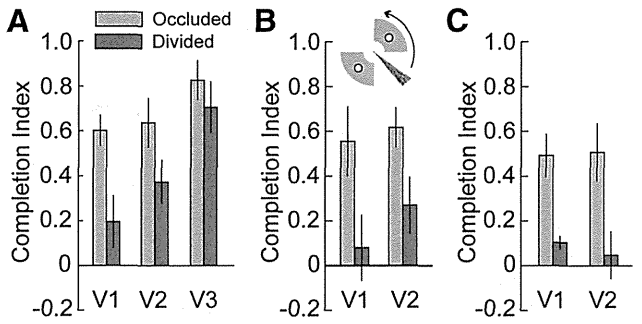

Figure 8. Completion indices in retinotopic ROIs for the occluded and divided stimuli. ***A***, Completion indices in retinotopic ROIs. The indices for the occluded stimulus revealed that only V1 and V2 exhibited significant completion-related activity compared with the divided stimulus. ***B***, Completion indices within the strictly limited regions in V1 and V2 corresponding to the middle position of the occluders. ***C***, Completion indices in retinotopic ROIs after excluding all voxels that showed responses at $p < 0.05$ level for the divided condition to minimize BOLD spread effects in the results. The voxel exclusion was done in each scanning day and each participant separately. Error bars, SEM.

negative responses corresponding to the target rotation, if observed, would generally work to inhibit completion-related activities. By putting effect of these potential relative phase shift into the index, we can avoid this problem and evaluate amodal responses more precisely in the next analysis.

Even after the voxel response phases were taken into account, V1 and V2 ROIs (but not V3 in this analysis (paired t test; $t_{(7)} = 1.25$, $p = 0.13$) exhibited significantly higher responses to the occluded than to the divided stimulus (paired t test; $t_{(7)} = 2.75$, $p = 0.014$ in V1; $t_{(7)} = 2.96$, $p = 0.011$ in V2; significant at $p < 0.05$ level after Bonferroni correction; Fig. 8*A*). The result indicates that V1 and V2 contribute to topographic amodal completion by boosting activities for the occluded and invisible visual object. This finding also indicates that neural responses to the amodal and real surfaces have relatively similar profiles. The indices for the occluded stimulus were 0.60 in V1 and 0.64 in V2. In contrast, although the indices for the divided stimulus were above zero level (paired t test; $t_{(7)} = 8.67$, $p = 0.000027$ in V1; $t_{(7)} = 5.77$, $p = 0.00034$ in V2; $t_{(7)} = 9.35$, $p = 0.000016$ in V3, uncorrected), their magnitudes (0.19 in V1 and 0.37 in V2) were significantly lower compared with the occluded stimulus. The amodal completion-related responses in V1 and V2 were robust even when the ROIs were strictly confined within the center positions of the occluders as a further defense against BOLD spread (paired t test, $t_{(7)} = 3.72$, $p = 0.0037$ in V1; $t_{(7)} = 3.50$, $p = 0.005$ in V2; Fig. 8*B*). Furthermore, to omit effects of BOLD spreads from the foveal and peripheral visible parts of the target stimulus more strictly, we excluded any voxels that showed significant responses (voxelwise Fourier F test, $p < 0.05$ uncorrected) for the divided stimulus from the analysis. Even after this strict limitation of voxels, V1/V2 completion-related activities were clear as shown in Figure 8*C* (paired t test; $t_{(7)} = 4.28$, $p = 0.0036$ in V1; $t_{(7)} = 3.8567$, $p = 0.0063$ in V2; significant at $p < 0.05$ level after Bonferroni correction), indicating robustness of the completion-related activity within exactly the retinotopic positions of the visual occlusion.

In foveal/peripheral regions of ROIs, no significant difference in the index was observed between conditions (paired t test; $p > 0.10$ for all the ROIs; Fig. 9*A*). This result also suggests that the effects of BOLD spreads from the outer regions into centers of ROIs would be minimal since as otherwise some differences would be also observed in the outer regions; if responses for the occluded stimulus at the occluding borders are high enough to modulate the activities in the ROIs, it would also affect the response profiles in the outer regions. Therefore, we can conclude that the neural modulation by an amodal surface is spatially limited to regions corresponding to the missing portion of an occluded object. Our previous fMRI study (Ban et al., 2006) found enhancement of retinotopic neural responses to a visible portion of a target stimulus when another stimulus was simultaneously presented to form a global structure even if they were presented relatively far apart in visual field. However, this type of response

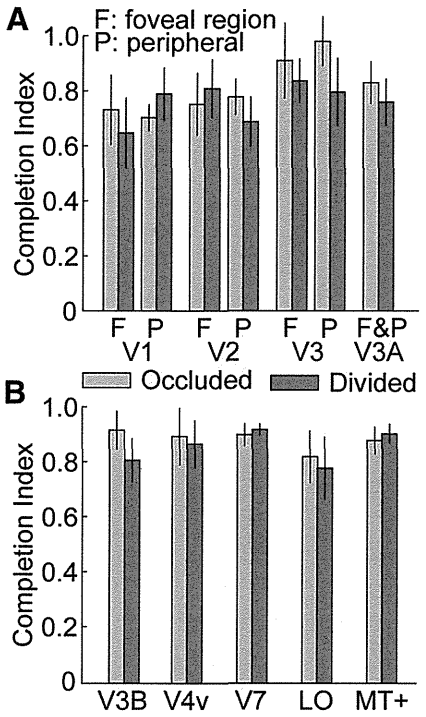

Figure 9. Completion indices in the outer regions of retinotopic ROIs and higher regions. ***A***, Completion indices in the foveal/peripheral outer regions of the target subregions that retinotopically represent the occluder positions. ***B***, The indices in coarsely retinotopic higher visual areas. Error bars, SEM.

modulation to the visible portions of the partially occluded target was not observed in this study. Thus, neural modulation by amodal completion in early visual areas appears to operate in such a fashion as to simply bridge the occluded portion.

No significant difference was observed in coarsely retinotopic higher areas (paired t test; $p > 0.10$ for all the ROIs; Fig. 9*B*). This was probably due to limitations of spatial resolution of fMRI, since BOLD spread is larger in higher visual areas, and to insensitivity of our retinotopy-based analysis for coarsely retinotopic higher areas. Alternatively, it is also possible that, with our stimulus configuration, these areas do not contribute to topographic completion of an occluded surface, or that they realize more global completion even for a divided target based on synchronized movements of visual elements or visual imagery. Further analysis, though it is beyond the scope of this study, is needed to reach clear conclusions.

Effects of temporally preceding cognitive context

The final question we attempted to answer is whether the observed neural representation of an occluded object is modulated by temporally preceding cognitive context, such as knowledge of the complete appearance of an object obtained before partial occlusion. Answering this question is important for understanding how the brain uses not only spatial (low-level image features) but also cognitive context in maintaining object consistency.

To this end, we presented the divided target rotation with two stable opaque occluders (Fig. 10*A*, nonoccluded condition). In this configuration, when the target rotated and passed through one of the occluders, the spatial alignments at the overlapping edges such as T-shaped junctions strongly enhanced the impression of occlusion, as in the occluded condition. However, an observer seeing the sequence of target rotation knows that the target is divided, and not occluded by the occluder. Temporally preceding cognitive experience thus reduces the impression of target occlusion. We explored how this type of incongruent stimulus configuration modulates early topographic responses. We focused on the activity in V1 and V2 in the analysis because reliable amodal completion-related activity was observed only in these areas (Fig. 8*A–C*).

Responses to this incongruent stimulus mapped on the inflated cortical surface suggested that the temporally preceding cognitive context appeared to have suppressive effect on completion-related activity (Fig. 10*B*), suggesting in turn that, contrary to common belief, early completion-related activity is not necessarily due to low-level image features alone.

Interestingly, further voxel-by-voxel detailed analyses showed that the response suppression by the cognitive context was only observed in the earliest visual area, V1. Voxel-by-voxel phase scatter-plots revealed that response profiles for the nonoccluded condition were similar with those of the transparent in V1 and V2, whereas periodic powers of the nonoccluded were lower than the transparent especially in V1 (Fig. 10*C*). Relative periodicity analysis (the occluded periodicity was divided by the nonoccluded one) revealed that neural responses in V1 was indeed suppressed by the temporally preceding cognitive context (t test whether the relative periodicity is >1; $t_{(7)} = 2.75, p = 0.014$ in V1; $t_{(7)} = 2.19, p = 0.032$ in V2, only V1 was significant at $p < 0.05$ level after Bonferroni correction; Fig. 10*D*). Furthermore, one-way (visual polar angles, six locations) repeated-measures ANOVA revealed no main effect of visual field location ($F_{(5,30)} = 0.30, p = 0.91$ in V1; $F_{(5,35)} = 1.80, p = 0.14$ in V2), indicating that cognitive suppression was observed even after the target was completely behind the occluder, and that the results obtained were not due to local differences in stimuli when the target entered the occluder (Fig. 10*E*).

To assess the cognitive effect in a more conservative fashion, we calculated completion indices. The indices for the nonoccluded condition were significantly lower than those for the occluded only in V1 but not in V2 (paired t test, $t_{(7)} = 9.85, p = 0.000012$ in V1; $t_{(7)} = 0.19, p = 0.43$ in V2, only V1 was significant at $p < 0.05$ level after Bonferroni correction; Fig. 11*A*). These profiles in V1 and V2 were robust even when the ROIs were strictly confined within the center positions of the occluders (but statistically marginally significant in this case; paired t test, $t_{(7)} = 1.52, p = 0.086$; Fig. 11*B*). Furthermore, when we analyzed data after excluding any voxels that showed $p < 0.05$ for the divided stimulus, the index for the nonoccluded was again statistically lower than the occluded only in V1 but not in V2 (paired t test; $t_{(7)} = 3.21, p = 0.014$ in V1; $t_{(7)} = 0.50, p = 0.63$ in V2; only V1 was significant at $p < 0.05$ level after Bonferroni correction; Fig. 11*C*). These results may suggest that observer's prior knowledge does modulate early neural completion-related activity. For indices in foveal/peripheral regions of ROIs, no significant difference was observed between conditions (paired t test, $p > 0.09$ for all regions; Fig. 11*D*).

Interestingly, the higher cognitive effect was found to be stronger in V1 than V2, suggesting that these areas play different roles in solving the occlusion problem; V1 might participate in feedback loops for integrating cognitive context, whereas V2 might be essential for analysis of local image features, such as T-shaped junctions. This discrepancy of response profiles between V1 and V2, together with a case study of patient LG (Gilaie-Dotan et al., 2009), gives a new insight into cortical occlusion representation. LG has abnormal function of intermediate visual areas (V2–V4) whereas fMRI response patterns in V1 and LOC

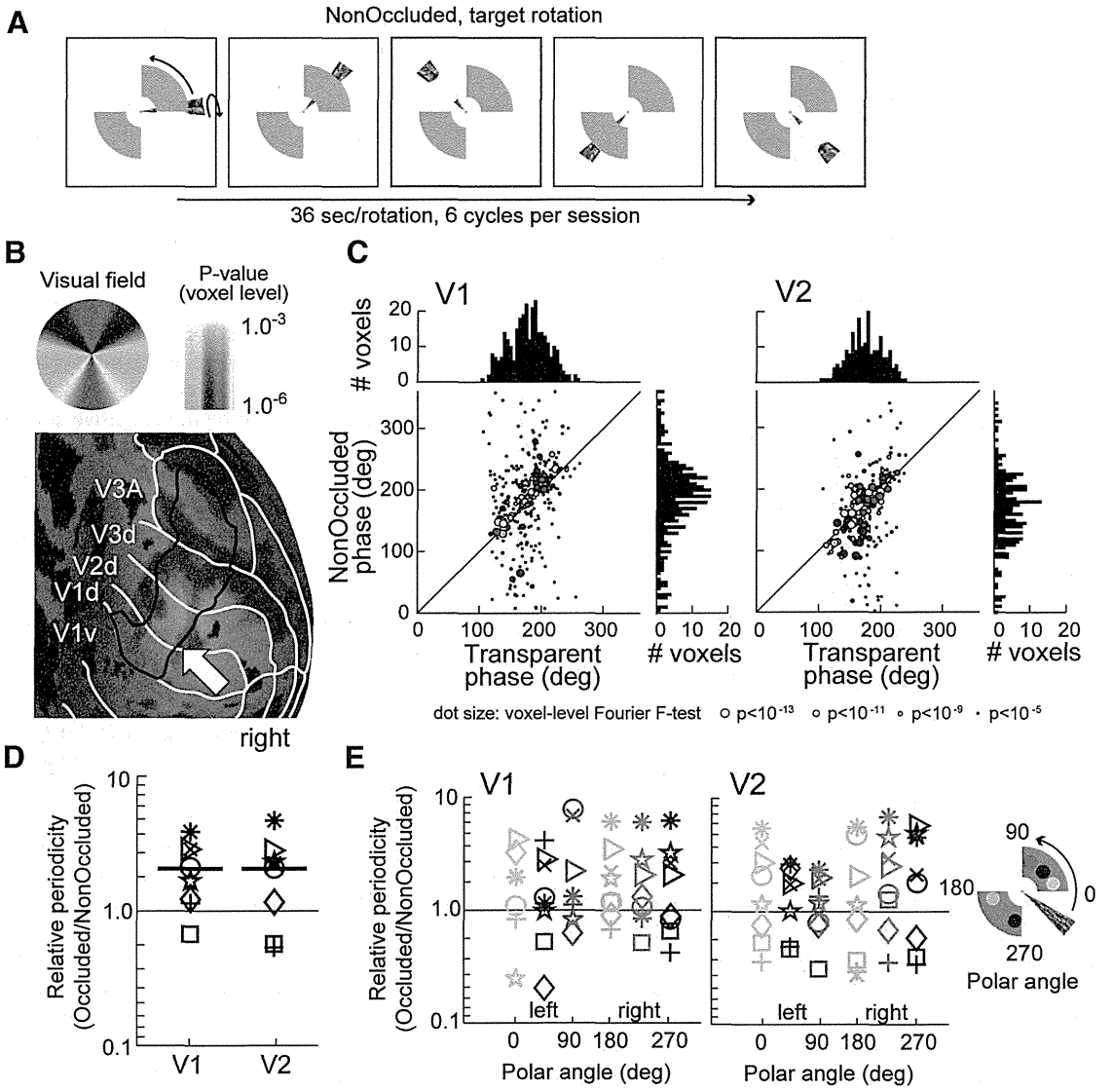

Figure 10. Effect of temporally preceding cognitive context on amodal completion-related activity. ***A***, Schematic view of the nonoccluded stimulus presentation. In this configuration, the divided target rotated so as to overlap two stable occluders. Therefore, an observer knows that the target is not occluded but divided, whereas spatial image features such as T-junctions promotes amodal completion percept. ***B***, Cortical activity in response to the nonoccluded stimulus. ***C***, Voxelwise phase scatter plots, transparent versus nonoccluded. Each color represents a single participant. Dot sizes represent magnitudes of Fourier *F*-statistics (and the corresponding statistical *p* values). For details, see Figure 5. ***D***, Relative periodicities (occluded/nonoccluded) exhibited significant decrease in V1 due to temporally preceding cognitive context. Each shape represents a single participant. ***E***, Comparison of relative periodic responses (occluded/nonoccluded) in V1 and V2 along polar angle representation. Each color represents the corresponding visual field location. Each shape represents a single participant.

seem to be normal. He has severe deficits with integrating collinear contours and recognizing occluded objects. From this point of view, cortical representations in intermediate levels of the visual processing as well as V1 may be required to solve visual occlusion. Alternatively, it may be possible that relatively local feedback signals (e.g., from V2–V4 to V1) as well as modulations from higher visual areas (see Discussion) would be essential for object completion. It would be worth investigating whether patients with lesions in V2–V4 show topographic neural representation of occlusion in V1.

Attention control experiment and control analyses

The observed topographic activity corresponding to the occluded portion may be alternatively explained as a result of object-based attention to the target (Somers et al., 1999; Mitchell et al., 2004; Lee and Vecera, 2005; Bressler and Silver, 2010; Pratte et al., 2013), or spatial attention to the locations of the occluders (Sasaki et al., 2001; Slotnick et al., 2005). To rule out these possibilities, we conducted an additional control experiment using the same stimuli (occluded and divided conditions only) and presentation procedures but with interposing a more difficult attention-demanding task on the central fixation point (see Materials and Methods). As shown in Figure 12, when controlling observer's attention more strictly, the absolute values of the completion index were lower than those of the main experiment (Fig. 8). However, we could still find the significantly higher completion indices for the occluded than the divided in V1/V2 and also in V3 in this experiment (Fig. 12*A*; paired *t* test; $t_{(7)} = 5.70, p = 0.00073$ in V1; $t_{(7)} = 8.00, p = 0.000091$ in V2; $t_{(7)} = 3.88, p = 0.0061$ in V3; all ROIs were significant at $p < 0.05$ level after Bonferroni correction). In the foveal/peripheral regions of ROIs, no significant difference was observed (Fig. 12*B*; paired *t* test, $p > 0.10$, for all regions).

It is also possible that attention may work as a noise filter, selectively reducing irrelevant signals at the attended location

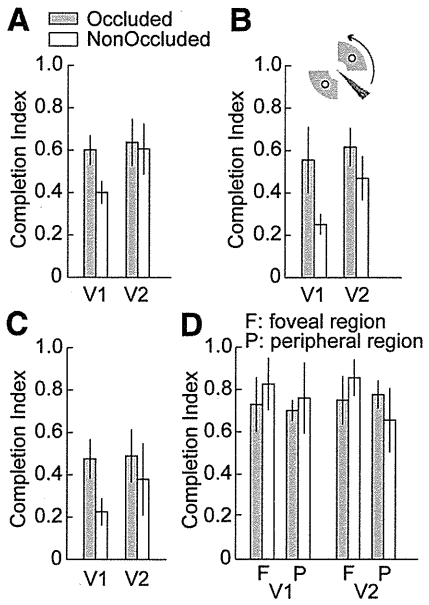

Figure 11. Completion indices for the occluded and nonoccluded stimuli. ***A***, Comparison of completion indices for the occluded and nonoccluded stimuli in V1 and V2. ***B***, Completion indices after the ROIs in V1/V2 were restricted to regions corresponding to the middle portion of the occluders. ***C***, Completion indices in V1 and V2 after excluding all voxels that showed responses at $p < 0.05$ level for the divided condition to minimize BOLD spread effects in the results. The voxel exclusion was done in each scanning day and each participant separately. ***D***, Completion indices in the foveal/peripheral regions of ROIs. Error bars, SEM.

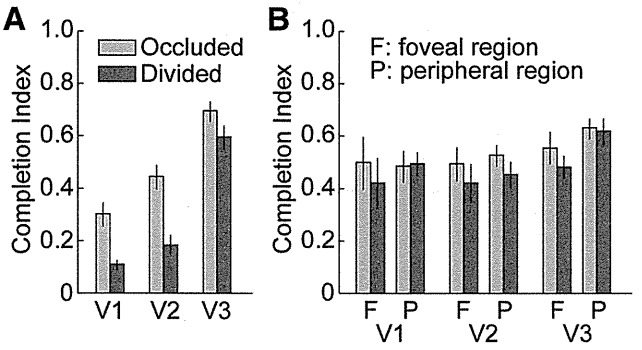

Figure 12. Completion indices for the occluded and divided stimuli with a more attention-demanding task. ***A***, Completion indices in retinotopic ROIs under an additional attention control experiment. Although the overall index values decreased in this experiment, higher indices for the occluded over the divided condition were again observed. ***B***, Completion indices in the foveal/peripheral regions of ROIs. Error bars, SEM.

(Dosher and Lu, 2000; Lu et al., 2002; Pratte et al., 2013). If this happened in our experiment and the overall noise level for the occluded condition was reduced over the divided and nonoccluded conditions, it would result in apparent response enhancement even without any occlusion completion-related signals. This is because Fourier *F*-statistics were computed by dividing the squared amplitude of power at the target rotation frequency (1/36 Hz) with the sum of squared amplitudes at the other frequencies. To rule out this possibility, we compared noise levels (averages of powers at all the frequencies other than the target rotation frequency and higher harmonics) of time series in each ROI across stimulus conditions in the main experiment. As shown in Figure 13, the results confirmed that the completion-like responses we found in the main experiment cannot be simply explained by overall noise reductions for the occluded condition. We could not observe any noise level differences across stimulus conditions both in the ROIs (Fig. 13*A*; repeated-measures ANOVA; ROI × stimulus condition; no main effect of stimulus condition, $F_{(2,14)} = 0.076$, $p = 0.93$) and in their foveal/peripheral outer regions (Fig. 13*B*; repeated-measures ANOVA ROI × inner/outer position × stimulus condition; no main effect of stimulus condition, $F_{(2,14)} = 0.13$, $p = 0.88$). We also compared the noise levels for the fMRI time series obtained with a more attention-demanding task (the occluded and divided conditions only). Again, no difference across stimulus conditions was observed both in the ROIs (Fig. 14*A*; repeated-measures ANOVA; ROI × stimulus condition; no main effect of stimulus condition, $F_{(1,7)} = 0.30$, $p = 0.60$) and in the foveal/peripheral regions (Fig. 14*B*; repeated-measures ANOVA; ROI × inner/outer position × stimulus condition; no main effect of stimulus condition, $F_{(1,7)} = 0.79$, $p = 0.40$).

From these results, we can conclude that the observed V1/V2 activity reflects neural amodal completion of the occluded portion. In addition, for all stimulus conditions, we imposed no attentional task related to target rotation and also no task on the location of the occluders. These facts together indicate that the observed topographic activity found here cannot be simply explained by an attention effect alone. Recent neuroimaging studies have also shown association between activity from early/higher visual areas and behavior performance even when the effects of attention were controlled (Sasaki and Watanabe, 2004; Meng et al., 2005; Ban et al., 2006, 2012). Furthermore, as shown in Figure 9*B*, response boosts could not be observed in the external regions of the occluding portions. Therefore, the observed completion responses would not be due to overall attention differences across stimuli and scanning runs. Finally, the observed discrepancy in the responses between V1 and V2 induced by the nonoccluded stimulus (Fig. 11) should not be attributed to simple attentional boosts in early visual areas.

However, we have to keep in mind that it is never entirely possible to completely rule out visuospatial attentional factors from the results. If we imposed an even more challenging fixation task, the withdrawal of attention from the occluded stimulus could also diminish perceptual grouping or binding of the two visible portions of the stimulus even more, resulting in reducing the topographic representation of the whole object in V1/V2. This is consistent with our finding that the knowledge whether the object is divided or whole is relevant to the completion responses. Therefore, although completion-related activity is actually observed, we cannot possibly make a firm conclusion that the completion is derived by an attention-free mechanism. It is not an exclusive scenario; knowing an object is occluded may guide attention to the occluded portion, or attention to the occluded portion may help bind the fragments into a coherent whole.

Discussion

Utilizing dynamically induced occlusion stimuli and investigating concurrent periodic shifts in fMRI activity in early visual cortex, the present study has provided clear human neuroimaging evidence for topographic representation of visual occlusion. We found that V1 and V2 exhibit topographic moment-to-moment activity corresponding to the occluded portion of an object. Based on detailed voxel-by-voxel analysis, we further demonstrated spatial specificity of neural modulation for an amodal object in multiple visual areas. The results of an additional control experiment confirmed that the observed topographic activity cannot be simply explained by attentional boosts of responses in early visual areas. Furthermore, we demonstrated